Chapter 10

Elastostatics

10.1 Introduction

In this chapter we consider static equilibria of elastic solids. Our first concern is to generalize Hooke's law, derived initially for weights hanging on thin wires, to accommodate three dimensional stress. The most appropriate mathematical machinery for continuum mechanics involves tensors and their derivatives. In particular, 3-dimensional deformations and the stresses they produce will be described by a second-rank *strain tensor* and a second-rank *stress tensor*. These will allow us to describe deformations and stresses in three dimensional solids of irregular shape. We will then develop a formalism to derive stresses from strains and *vice versa* and will illustrate it by application to the problems of thermoelastic noise in gravitational-wave detectors, large telescope mirrors, cantilever bridges, and mountains.

This standard approach to elasticity is our first example of a common (some would complain far too common) approach to a physics problem, namely to linearize it. Linearization may be acceptable when the distortions are small. However, under strong loading, elastic media may become neutrally stable to small displacements which can therefore grow to large amplitude. A classical result of elasticity theory, due originally to Euler, is that when an elastic solid is compressed, there comes a point where stable equilibria can disappear. For an applied force in excess of this maximum, the solid will *buckle*. This is an example of *bifurcation*, a phenomenon, as has subsequently been realized, that is common to many physical systems. We will illustrate bifurcation using a strut under a compressive load. We will encounter other examples of bifurcation when we study fluids, in Part IV of the book.

10.2 Strain; Expansion, Rotation, and Shear

From the point of view of continuum mechanics, a *solid* is a substance that recovers its shape after the application and removal of *any* small stress. That is to say, after the stress is removed, the solid can be rotated and translated to assume its original shape. Note the requirement that this be true for any stress. Many fluids (e.g. water) are effectively incompressible. This means that they satisfy our definition as long as the applied stress is isotropic; however, they will deform permanently under a shear stress. Other materials (for example, the earth's crust) are only elastic for limited times, but undergo plastic flow when a stress is applied for a long time.

We shall confine our attention to *elastic solids* which deform while the stress is being applied in such a way that the magnitude of the deformation is linearly proportional to the applied force. This generalizes Hooke's famous law (originally expressed in the concise Latin phrase "*Ut tensio, sic vis*"). This law naturally implies that the deformation vanishes when the force is removed. Before imposing this linear relationship, we must first introduce a formalism to measure the deformation (the strain) and the applied force (the stress) and the relationship between them. We shall insist—in accord with the philosophy introduced in Chapter 1—that the strain, the stress, and their relationship be described in geometric, coordinate-independent language. By doing so, we shall achieve considerable power.

10.2.1 Strain Tensor

First, let us describe the deformation. We label the position of a point in an unstressed body relative to some convenient origin in the body, by a position vector $\mathbf{x}$. Now, let a force be applied so that the body deforms and the position vector changes $\mathbf{x} \to \mathbf{x} + \boldsymbol{\xi}(\mathbf{x})$, where $\boldsymbol{\xi}$ is the *displacement vector*. If $\boldsymbol{\xi}$ were constant (i.e., if its components in a Cartesian coordinate system were independent of location in the body), then the body would simply be translated and would undergo no deformation. To produce a deformation, we must make the displacement $\boldsymbol{\xi}$ change from one location to another. The most simple, *coordinate-independent* way to quantify those changes is by the *gradient* of $\boldsymbol{\xi}$, $\boldsymbol{\nabla\xi}$. This gradient is a second-rank tensor field; we shall give it the name *strain tensor* and shall denote it $\mathbf{S}$:

$$\mathbf{S} = \boldsymbol{\nabla\xi} \; . \tag{10.1}$$

This strain tensor is a geometric object, defined independent of any coordinate system in the manner described in Sec. 1.8. In slot-naming index notation, it is denoted

$$S_{ij} = \xi_{i;j} \; , \tag{10.2}$$

where the index j after the semicolon is the name of the gradient slot.

In a Cartesian coordinate system the components of a gradient are always just partial derivatives [Eq. (1.87)], and therefore the Cartesian components of the strain tensor are

$$S_{ij} = \frac{\partial \xi_i}{\partial x_j} = \xi_{i,j} \; . \tag{10.3}$$

(Recall that indices following a comma represent partial derivatives.) In the next section we shall learn how to compute the components of the strain in cylindrical and spherical coordinates.

In any small neighborhood of any point $\mathcal{P}$ in a deformed body, we can reconstruct the displacement vector $\boldsymbol{\xi}$ from the strain tensor, up to an additive constant. In Cartesian coordinates centered on $\mathcal{P}$, by virtue of a Taylor series expansion, $\boldsymbol{\xi}$ is given by

$$\xi_i(\mathbf{x}) = x_j(\partial \xi_i/\partial x_j) + \dots \; , \tag{10.4}$$

where we have set to zero the value of $\boldsymbol{\xi}$ at $\mathcal{P}$ (the additive constant). Discarding quadratic and higher-order terms, and using $S_{ij} = \xi_{i,j}$, we can rewrite Eq. (10.4) as

$$\xi_i = S_{ij} x_j \ . \tag{10.5}$$

We have derived this as a relationship between components of $\boldsymbol{\xi}$, $\mathbf{x}$, and $\mathbf{S}$ in a Cartesian coordinate system. However, the indices can also be thought of as the names of slots, and correspondingly Eq. (10.5) can be regarded as a geometric, coordinate-independent relationship between the vectors and tensor $\boldsymbol{\xi}$, $\mathbf{x}$, and $\mathbf{S}$.

In Box 10.2.1 we introduce the concept of the *irreducible tensorial parts* of a tensor, and we state that in physics, whenever one encounters a new, unfamiliar tensor, it is often useful to identify the tensor's irreducible parts. The strain tensor $\mathbf{S}$ is an important example. It is a general, second-rank tensor. Therefore, as we discuss in 10.2.1, its irreducible tensorial parts are its trace Θ, which is called the deformed body's *expansion* for reasons we shall explore below; its symmetric, trace-free part $\boldsymbol{\Sigma}$, which is called the body's *shear*; and its antisymmetric part $\mathbf{R}$, which is called the body's *rotation*:

$$\begin{aligned} \Theta &= S_{ii} \ , \\ \Sigma_{ij} &= \frac{1}{2}(S_{ij} + S_{ji}) - \frac{1}{3}\Theta g_{ij} \ , \\ R_{ij} &= \frac{1}{2}(S_{ij} - S_{ji}) \ . \end{aligned} \tag{10.6}$$

The strain tensor can be reconstructed from these irreducible tensorial parts in the following manner [Eq. (4) of Box 10.2.1, rewritten in abstract notation]:

$$\boldsymbol{\nabla}\boldsymbol{\xi} = \mathbf{S} = \frac{1}{3}\Theta\mathbf{g} + \boldsymbol{\Sigma} + \mathbf{R}. \tag{10.7}$$

Let us consider the effects of the three separate parts of $\mathbf{S}$ in turn. To understand expansion, consider a small 3-dimensional piece $\mathcal{V}$ of a deformed body (a "volume element"). The change in the volume element's volume, produced by the displacement field $\boldsymbol{\xi}$, can be computed from the displacement of its surface $\partial\mathcal{V}$ as

$$\delta V = \int_{\partial\mathcal{V}} d\mathbf{\Sigma} \cdot \boldsymbol{\xi} = \int_{\mathcal{V}} dV \boldsymbol{\nabla} \cdot \boldsymbol{\xi} \tag{10.8}$$

where we have invoked Gauss' theorem. (Note that we use $\mathbf{\Sigma}$ for a surface vector and $\boldsymbol{\Sigma}$ for a strain tensor. There should be no confusion.) Therefore in the limit that $V \to 0$,

$$\Theta = \boldsymbol{\nabla} \cdot \boldsymbol{\xi} \simeq \frac{\delta V}{V} \tag{10.9}$$

The expansion, therefore, is simply the fractional change in volume of a small region of the solid; see Figure 10.1 for a simple example.

The shear tensor $\boldsymbol{\Sigma}$ produces the shearing displacements illustrated in Figures 10.1 and 10.2. As it has zero trace, there is no volume change when a body undergoes a pure shear deformation. The shear tensor has five independent components. However, by rotating our

Box 10.1
Irreducible Tensorial Parts of a Second-Rank Tensor in 3-Dimensional Euclidean Space

In quantum mechanics an important role is played by the "rotation group," i.e., the set of all rotation matrices viewed as a mathematical entity called a group; see, e.g., chapter XIII of Messiah (1962) or chapter 16 of Mathews and Walker (1965). Each tensor in 3-dimensional Euclidean space, when rotated, is said to generate a specific "representation" of the rotation group. Tensors that are "big", in a sense to be discussed below, can be broken down into a sum of several tensors that are "as small as possible." These smallest tensors are said to generate "irreducible representations" of the rotation group. All this mumbo-jumbo is really very simple, when one thinks about tensors as geometric, frame-independent objects.

As an example, consider an arbitrary second-rank tensor S_{ij} in three-dimensional, Euclidean space. In the text S_{ij} will be the strain tensor. From this tensor we can construct the following "smaller" tensors by linear operations that involve only S_{ij} and the metric g_{ij}. (As these smaller tensors are enumerated, the reader should think of the notation used as basis-independent, frame-independent, slot-naming index notation.) The smaller tensors are the "trace" of S_{ij},

$$\Theta \equiv S_{ij} g_{ij} = S_{ii} \; ; \tag{1}$$

the antisymmetric part of S_{ij}

$$R_{ij} \equiv \frac{1}{2}(S_{ij} - S_{ji}) \; ; \tag{2}$$

and the symmetric, trace-free part of S_{ij}

$$\Sigma_{ij} \equiv \frac{1}{2}(S_{ij} + S_{ji}) - \frac{1}{3} g_{ij} S_{kk} \; . \tag{3}$$

It is straightforward to verify that the original tensor S_{ij} can be reconstructed from these three "smaller" tensors, plus the metric as follows:

$$S_{ij} = \Sigma_{ij} + \frac{1}{3}\Theta g_{ij} + R_{ij} \; . \tag{4}$$

One way to see the sense in which Θ, R_{ij}, and Σ_{ij} are "smaller" than S_{ij} is by counting the number of independent real numbers required to specify their components in an arbitrary basis. (In this counting the reader is asked to think of the index notation as components on the chosen basis.) The original tensor S_{ij} has $3 \times 3 = 9$ components $(S_{11}, S_{12}, S_{13}, S_{21}, \ldots)$, all of which are independent. By contrast, the 9 components of Σ_{ij} are not independent; symmetry requires that $\Sigma_{ij} \equiv \Sigma_{ji}$, which reduces the number of independent components from 9 to 6 and trace-freeness, $\Sigma_{ii} = 0$ reduces it further from 6 to 5. The antisymmetric tensor R_{ij} has just three independent components, R_{12}, R_{23},

Box 10.1, Continued

and R_{31}. The scalar Θ has just one. Note that (5 independent components in Σ_{ij}) + (3 independent components in R_{ij}) + (1 independent components in Θ) = 9 = (number of independent components in S_{ij}).

The number of independent components (one for Θ, 3 for R_{ij}, 5 for Σ_{ij}) is a geometric, basis-independent concept: It is the same, regardless of the basis used to count the components; and for each of the "smaller" tensors that make up S_{ij}, it is easily deduced without introducing a basis at all: (Here the reader is asked to think in slot-naming index notation.) The scalar Θ is clearly specified by just one real number. The antisymmetric tensor R_{ij} contains precisely the same amount of information as the vector

$$\phi_i \equiv -\frac{1}{2}\epsilon_{ijk} R_{jk} \ , \tag{5}$$

as one can see from the fact that Eq. (5) can be inverted to give

$$R_{ij} = -\epsilon_{ijk}\phi_k \ ; \tag{6}$$

and the vector ϕ_i can be characterized by its direction in space (two numbers) plus its length (a third). The symmetric, trace-free tensor Σ_{ij} can be characterized geometrically by the ellipsoid $(g_{ij} + \varepsilon\Sigma_{ij})\zeta_i\zeta_j = 1$, where ε is an arbitrary number $\ll 1$ and ζ_i is a vector whose tail sits at the center of the ellipsoid and head moves around on the ellipsoid's surface. Because Σ_{ij} is trace-free, this ellipsoid has unit volume. It therefore is specified fully by the direction of its longest principal axis (two numbers) plus the direction of a second principle axis (a third number) plus the ratio of the length of the second axis to the first (a fourth number) plus the ratio of the length of the third axis to the first (a fifth number).

Each of the tensors Θ, R_{ij} (or equivalently ϕ_i), and Σ_{ij} is "irreducible" in the sense that one cannot construct any "smaller" tensors from it, by any linear operation that involves only it, the metric, and the Levi-Civita tensor. Irreducible tensors always have an odd number of components. It is conventional to denote this number by $2l+1$ where the integer l is called the "order of the irreducible representation of the rotation group" that the tensor genenerates. For Θ, R_{ij} (or equivalently ϕ_i), and Σ_{jk}, l is 0, 1, and 2 respectively. These three tensors can be mapped into the spherical harmonics of order $l = 0,\ 1,\ 2$; and their $2l+1$ components correspond to the $2l+1$ values of the quantum number $m = -l,\ -l+1\ \ldots\ , l-1,\ l$. For details see, e.g., section II.C of Thorne (1980).

In physics, when one encounters a new, unfamiliar tensor, it is often useful to identify the tensor's irreducible parts. They almost always play important, independent roles in the physical situation one is studying. We shall meet one example in this chapter, and another when we study fluid mechanics (Part IV).

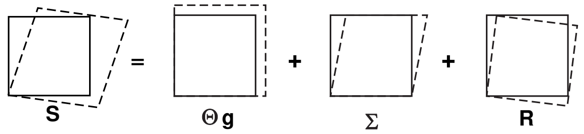

Fig. 10.1: A simple example of the decomposition of a two dimensional distortion of a lattice into an expansion (Θ), a shear ($\boldsymbol{\Sigma}$), and a rotation ($\mathbf{R}$).

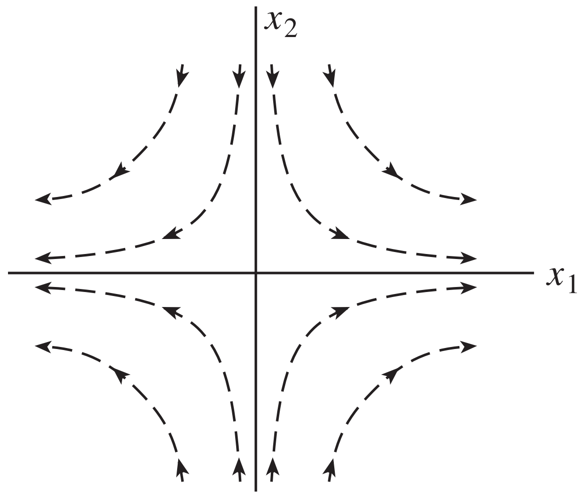

Fig. 10.2: Shear in two dimensions. The displacement of points in a solid undergoing pure shear is the vector field $\boldsymbol{\xi}(\mathbf{x})$ given by Eq. (10.5) with S_{ji} replaced by Σ_{ji}: $\xi_j = \Sigma_{ji}x_i = \Sigma_{j1}x_1 + \Sigma_{j2}y$. The integral curves of this vector field are plotted in this figure. The figure is drawn using principal axes, which are Cartesian, so $\Sigma_{12} = \Sigma_{21} = 0$, $\Sigma_{11} = -\Sigma_{22}$, which means that $\xi_1 = \Sigma_{11}x_1$, and $\xi_2 = -\Sigma_{11}y$. The integral curves of this simple vector field are the hyperbolae shown in the figure. Note that the displacement increases linearly with distance from the origin.

Cartesian coordinates appropriately, we can transform away all the off diagonal elements, leaving the three diagonal elements, which must sum to zero. This is known as a *principal axis transformation*. The components of the shear tensor in a cartesian coordinate system can be written down immediately from Eq. (10.6) by substituting the Kronecker delta δ_{ij} for the metric tensor g_{ij} and treating all derivatives as partial derivatives:

$$\Sigma_{xx} = \frac{2}{3}\frac{\partial \xi_x}{\partial x} - \frac{1}{3}\left(\frac{\partial \xi_y}{\partial y} + \frac{\partial \xi_z}{\partial z}\right) , \quad \Sigma_{xy} = \frac{1}{2}\left(\frac{\partial \xi_x}{\partial y} - \frac{\partial \xi_y}{\partial x}\right) , \tag{10.10}$$

and similarly for the other components. The analogous equations in spherical and cylindrical coordinates will be described in the next section.

The third term in Eq. (10.7) describes a pure rotation which does not deform the solid. To verify this, write $\boldsymbol{\xi} = \boldsymbol{\phi} \times \mathbf{x}$ where $\boldsymbol{\phi}$ is a small rotation of magnitude ϕ about an axis parallel to the direction of $\boldsymbol{\phi}$. Using cartesian coordinates in three dimensional Euclidean space, we can demonstrate by direct calculation that the symmetric part of $\mathbf{S}$ vanishes, i.e., $\Theta = \boldsymbol{\Sigma} = 0$ and that

$$R_{ij} = -\epsilon_{ijk}\phi_k , \qquad \phi_i = -\frac{1}{2}\epsilon_{ijk}R_{jk} . \tag{10.11}$$

Therefore the elements of the tensor $\mathbf{R}$ in a cartesian coordinate system just involve the angle $\boldsymbol{\phi}$. Note that expression (10.11) for $\boldsymbol{\phi}$ and expression (10.7) for R_{ij} imply that $\boldsymbol{\phi}$ is half the curl of the displacement vector,

$$\boldsymbol{\phi} = \frac{1}{2}\boldsymbol{\nabla} \times \boldsymbol{\xi} \, . \tag{10.12}$$

A simple example of rotation is shown in the last picture in Figure 10.1.

Let us consider some examples of strains that can arise in physical systems.

(i) Understanding how materials deform under various loads is central to mechanical, civil and structural engineering. As we have already remarked, in an elastic solid, the deformation (i.e. strain) is proportional to the applied stress. If, for example, we have some structure of negligible weight and it supports a load, then the amount of strain will increase everywhere in proportion to this load. However this law will only be obeyed as long as the strain is sufficiently small that the material out of which the structure is constructed behaves elastically. At a large enough strain, plastic flow will set in and the solid will not return to its original shape after the stress is removed. The point where this happens is known as the *elastic limit*. For a *ductile* substance like polycrystalline copper with a relatively low elastic limit, this occurs at strains $\sim 10^{-4}$. (However, failure will not occur until the *yield point* which occurs at a strain $\sim 10^{-3}$.) For a more resilient material like cemented tungsten carbide, strains can be elastic up to $\sim 3 \times 10^{-3}$, and for rubber, a non-Hookean material, recoverable strains of three or four are possible. What is significant is that all these strains (with the exception of that in rubber) are small, $\ll 1$. So, usually, when a material behaves elastically, the strains are small and the linear approximation is consequently pretty good.

(ii) Continental drift can be measured on the surface of the earth using Very Long Baseline Interferometry, a technique in which two or more radio telescopes are used to detect interferometric fringes using radio waves from a distant point source. (A similar technique uses the Global Positioning System to achieve comparable accuracy.) By observing the fringes, it is possible to detect changes in the spacing between the telescopes as small as a fraction of a wavelength ($\sim$ 10mm). As the telescopes are typically 1000km apart, this means that dimensionless strains $\sim 10^{-8}$ can be measured. Now, the continents drift apart on a timescale $\lesssim 10^8$yr., so it takes roughly a year for these changes to grow large enough to be measured. Such techniques are becoming useful for monitoring earthquake faults.

(iii) The smallest strains that have been measured so far involve laser interferometer gravitational-wave detectors. In prototype interferometers, two mirrors hang freely separated by $\sim$ 100m. Their separations can be monitored to better than $\sim 10^{-17}$m, one hundredth the radius of a nucleon! The associated strain is $\sim 10^{-19}$. In full-scale interferometers, which will go into operation in 2001, the separations are nearly a hundred times longer and the measured strains will be a hundred times smaller. Although these strains are measurements in vacuo and are not associated with an elastic solid, they do indicate the high accuracy of optical measurement techniques.

10.3 Cylindrical and Spherical Coordinates: Connection Coefficients and Components of Strain

Thus far, in our discussion of strain, we have resticted ourselves to Cartesian coordinates. However, many problems in elasticity are most efficiently solved using cylindrical or spherical coordinates, so in this section we shall develop some mathematical tools for those coordinate systems. In doing so we follow the vectorial conventions of standard texts on electrodynamics and quantum mechanics (e.g., Jackson 1999, and Messiah 1962): We introduce an *orthonormal* set of basis vectors associated with each of our curvilinear coordinate systems; the coordinate lines are orthogonal to each other, and the basis vectors have unit lengths and point along the coordinate lines. In our study of continuum mechanics (Part III – Elasticity, Part IV – Fluid Mechanics, and Part V – Plasma Physics), we shall follow this practice. Then in studying General Relativity and Cosmology (Part VI) we shall introduce and use basis vectors that are *not* orthonormal.

Our notation for cylindrical coordinates is (ϖ, ϕ, z); ϖ (pronounced "pomega") is distance from the z axis, and ϕ is angle around the z axis, so

$$\varpi = \sqrt{x^2 + y^2}\ , \quad \phi = \arctan(y/x)\ . \tag{10.13}$$

The unit basis vectors that point along the coordinate axes are denoted $\mathbf{e}_\varpi$, $\mathbf{e}_\phi$, $\mathbf{e}_z$, and are related to the Cartesian basis vectors by

$$\mathbf{e}_\varpi = (x/\varpi)\mathbf{e}_x + (y/\varpi)\mathbf{e}_y\ , \quad \mathbf{e}_\phi = -(y/\varpi)\mathbf{e}_x + (x/\varpi)\mathbf{e}_y\ , \quad \mathbf{e}_z = \text{Cartesian } \mathbf{e}_z\ . \tag{10.14}$$

Our notation for spherical coordinates is (r, θ, ϕ), with (as should be very familiar)

$$r = \sqrt{x^2 + y^2 + z^2}\ , \quad \theta = \text{arccot}(z/r)\ , \quad \phi = \arctan(y/x)\ . \tag{10.15}$$

The unit basis vectors associated with these coordinates are

$$\mathbf{e}_r = \frac{x}{r}\mathbf{e}_x + \frac{y}{r}\mathbf{e}_y + \frac{z}{r}\mathbf{e}_z\ , \quad \mathbf{e}_\theta = \frac{z}{r}\mathbf{e}_\varpi - \frac{\varpi}{r}\mathbf{e}_z\ , \quad \mathbf{e}_\phi = -\frac{y}{\varpi}\mathbf{e}_x + \frac{x}{\varpi}\mathbf{e}_y\ . \tag{10.16}$$

Because our bases are orthonormal, the components of the metric of 3-dimensional space retain the kronecker-delta values

$$g_{jk} \equiv \mathbf{e}_j \cdot \mathbf{e}_k = \delta_{jk}, \tag{10.17}$$

which permits us to keep all vector and tensor indices down, by contrast with spacetime where we must distinguish between up and down; cf. Sec. 1.5.[1]

In Jackson (1999), Messiah (1962) and other standard texts, formulas are written down for the gradient and Laplacian of a scalar field, and the divergence and curl of a vector field, in cylindrical and spherical coordinates; and one uses these formulas over and over again. In elasticity theory we deal largely with second rank tensors, and will need formulae for their

[1] Occasionally, e.g. in the useful equation $\epsilon_{ijm}\epsilon_{klm} = \delta^{ij}_{kl} \equiv \delta^i_k\delta^j_l - \delta^i_l\delta^j_k$ [Eq. (1.97)], it is convenient to put some indices up; but because $g_{jk} = \delta_{jk}$, any component with an index up is equal to that same component with an index down; e.g., $\delta^i_k \equiv \delta_{ik}$.

various derivatives in cylindrical and spherical coordinates. Rather than building up a huge table of such formulae, in this book we introduce a mathematical tool, *connection coefficients* Γ_{ijk}, by which they can be derived when needed.

The connection coefficients quantify the turning of the orthonormal basis vectors as one moves from point to point in Euclidean 3-space; i.e., they tell us how the basis vectors at one point in space are *connected to* (related to) those at another point. More specifically, we define Γ_{ijk} by the two equivalent relations

$$\nabla_k \mathbf{e}_j = \Gamma_{ijk}\mathbf{e}_i \; ; \quad \Gamma_{ijk} = \mathbf{e}_i \cdot (\nabla_k \mathbf{e}_j) \; ; \tag{10.18}$$

here $\nabla_k \equiv \nabla_{\mathbf{e}_k}$ is the directional derivative along the orthonormal basis vector $\mathbf{e}_k$; cf. Eq. (1.85). Notice that (as is true quite generally; cf. Sec. 1.9) the differentiation index comes *last* on Γ. Because our basis is orthonormal, it must be that $\nabla_k(\mathbf{e}_i \cdot \mathbf{e}_j) = 0$. Expanding this out using the standard rule for differentiating products, we obtain $\mathbf{e}_j \cdot (\nabla_k \mathbf{e}_i) + \mathbf{e}_i \cdot (\nabla_k \mathbf{e}_j)$. Then invoking the definition (10.18) of the connection coefficients, we see that Γ_{ijk} is antisymmetric on its first two indices:

$$\Gamma_{ijk} = -\Gamma_{jik} \; . \tag{10.19}$$

In Part VI, when we use non-orthonormal bases, this antisymmetry will break down.

It is straightforward to compute the connection coefficients for cylindrical and spherical coordinates from the definition (10.18), expressions (10.14) and (10.16) for the cylindrical and spherical basis vectors in terms of the Cartesian basis vectors, and from the fact that in Cartesian coordinates the connection coefficients vanish ($\mathbf{e}_x$, $\mathbf{e}_y$ and $\mathbf{e}_z$ do not rotate as one moves through Euclidean 3-space). One can also deduce the cylindrical and spherical connection coefficients by drawing pictures of the basis vectors and observing how they change from point to point. For cylindrical coordinates, we find that $\nabla_\phi \mathbf{e}_\varpi = \mathbf{e}_\phi/\varpi$ and $\nabla_\phi \mathbf{e}_\phi = -\mathbf{e}_\varpi/\varpi$. All other derivatives vanish. Hence,

$$\Gamma_{\varpi\phi\phi} = -\frac{1}{\varpi}, \quad \Gamma_{\phi\varpi\phi} = \frac{1}{\varpi} \; . \tag{10.20}$$

in agreement with Eq. (10.19). Likewise, for spherical coordinates

$$\Gamma_{\theta r\theta} = \Gamma_{\phi r\phi} = -\Gamma_{r\theta\theta} = -\Gamma_{r\phi\phi} = \frac{1}{r}, \quad \Gamma_{\phi\theta\phi} = -\Gamma_{\theta\phi\phi} = \frac{\cot\theta}{r} \; ; \tag{10.21}$$

The connection coefficients are the keys to differentiating vectors and tensors. Consider the strain tensor $\mathbf{S} = \boldsymbol{\nabla\xi}$. Applying the product rule for differentiation, we obtain

$$\nabla_k(\xi_j \mathbf{e}_j) = \xi_{j,k}\mathbf{e}_j + \xi_j \Gamma_{ljk}\mathbf{e}_l \tag{10.22}$$

Here the comma denotes the directional derivative, along a basis vector, of the components treated as scalar fields. So, for example, *in cylindrical coordinates* we have

$$\xi_{i,\varpi} = \frac{\partial \xi_i}{\partial \varpi} \; , \quad \xi_{i,\phi} = \frac{1}{\varpi}\frac{\partial \xi_i}{\partial \phi} \; , \quad \xi_{i,z} = \frac{\partial \xi_i}{\partial z} \; ; \tag{10.23}$$

and *in spherical coordinates* we have

$$\xi_{i,r} = \frac{\partial \xi_i}{\partial r} \; , \quad \xi_{i,\theta} = \frac{1}{r}\frac{\partial \xi_i}{\partial \theta} \; , \quad \xi_{i,\phi} = \frac{1}{r\sin\theta}\frac{\partial \xi_i}{\partial \phi} \; . \tag{10.24}$$

Taking the i'th component of Eq. (10.22) we obtain

$$S_{ik} = \xi_{i;k} = \xi_{i,k} + \Gamma_{ijk}\xi_j \ . \tag{10.25}$$

$\xi_{i;k}$ are the nine components of the gradient of the vector field $\boldsymbol{\xi}(\mathbf{x})$ evaluated in any orthonormal basis. We can use Eq. (10.25) , to evaluate the expansion $\theta \equiv \mathrm{Tr}\mathbf{S} \equiv \boldsymbol{\nabla}\cdot\boldsymbol{\xi}$. Using Eq. (10.20) , (10.21) , we obtain

$$\boldsymbol{\nabla}\cdot\boldsymbol{\xi} = \frac{\partial\xi_\varpi}{\partial\varpi} + \frac{1}{\varpi}\frac{\partial\xi_\phi}{\partial\phi} + \frac{\partial\xi_z}{\partial z} + \frac{\xi_\varpi}{\varpi} \ , \tag{10.26}$$

in cylindrical coordinates and

$$\boldsymbol{\nabla}\cdot\boldsymbol{\xi} = \frac{\partial\xi_r}{\partial r} + \frac{1}{r}\frac{\partial\xi_\theta}{\partial\theta} + \frac{1}{r\sin\theta}\frac{\partial\xi_\phi}{\partial\phi} + \frac{2\xi_r}{r} + \frac{\cot\theta\xi_\theta}{r} \ , \tag{10.27}$$

in spherical coordinates. So far, so good (cf. Jackson 1999).

Now we have the machinery for computing the complete gradient of a vector (cf. Box 10.3, we can go on to differentiate a second rank tensor $\mathbf{T} = T_{ij}\mathbf{e}_i \otimes \mathbf{e}_j$.

$$T_{ij;k} = T_{ij,k} + \Gamma_{ilk}T_{lj} + \Gamma_{jlk}T_{il} \ , \tag{10.28}$$

and so on. Equation (10.28) for the components of the gradient can be understood as follows: In cylindrical or spherical coordinates, the components T_{ij} can change from point to point as a result of two things: a change of the tensor $\mathbf{T}$, or the turning of the basis vectors. The two connection coefficient terms in Eq. (10.28) remove the effects of the basis turning, leaving in $T_{ij;m}$ only the influence of the change of $\mathbf{T}$ itself. There are two correction terms corresponding to the two slots (indices) of $\mathbf{T}$; the effects of basis turning on each slot get corrected one after another. If $\mathbf{T}$ had had n slots, then there would have been n correction terms, each with the form of the two in Eq. (10.28).

These expressions are not required to deal with the vector fields of introductory electromagnetic theory, but are essential to manipulate the tensor fields that are encountered in elasticity. As we shall see, in Part 6, with one further generalization, we can go on to differentiate tensors in any basis in a curved spacetime as is needed to perform calculations in general relativity.

****

EXERCISES

Exercise 10.1 *Derivation and Practice: Connection in Cylindrical Coordinates*

a. Draw a picture showing a cylindrical coordinate system and the orthonormal cylindrical basis vectors at neighboring locations. Use this picture to convince yourself that the only nonzero connection coefficients in this basis are $\Gamma_{\varpi\phi\phi}$ and $\Gamma_{\phi\varpi\phi}$, and to convince yourself that the values of these coefficients are as given in Eq. (10.20).

b. Use Eqs. (10.13) and (10.14) for the cylindrical coordinates and basis in terms of the Cartesian ones, and definition (10.18) for the connection coefficients, to derive expression (10.20) for $\Gamma_{\varpi\phi\phi} = -\Gamma_{\phi\varpi\phi}$.

Exercise 10.2 *Derivation and Practice: Expansion in Cylindrical and Spherical Coordinates*
Derive Eq. (10.26) ,(10.27) for the divergence of the vector field $\boldsymbol{\xi}$ in cylindrical and spherical coordinates using (10.20) and (10.21).

****

10.4 Stress and Elastic Moduli

10.4.1 Stress Tensor

The forces acting within an elastic solid are measured by a second rank tensor, the *stress tensor*—which is the spatial part of the stress-energy tensor that we met in Sec. 1.10. Let us recall the definition of this stress tensor:

Consider two small, contiguous regions in a solid. If we take a small element of area $d\boldsymbol{\Sigma}$ in the contact surface, then the first region exerts a force $d\mathbf{F}$ (not necessarily normal to the surface) on the second through this area. The force the second region exerts on the first will, by Newton's third law, be equal and opposite to this force. The force and the area of contact are both vectors and there is a linear relationship between them. (If we double the area, we double the force.) The two vectors therefore will be related by a second rank tensor, the stress tensor T:

$$d\mathbf{F} = \mathsf{T}\cdot d\boldsymbol{\Sigma} = \mathsf{T}(\ldots, d\boldsymbol{\Sigma}) \; . \tag{10.29}$$

(In index notation, $dF_i = T_{ij} d\Sigma_j$.) Note that the tensor T is the net force per unit area that a body exerts upon its surroundings. Be aware that many books on elasticity (e.g. Landau and Lifshitz) define the stress tensor with the opposite sign to (10.29). Also be careful not to confuse the shear tensor Σ_{jk} with the vectorial infinitesimal surface area $d\Sigma_j$.

We often need to compute the elastic force acting on some finite volume $\mathcal{V}$. Let us now make an important assumption, which we discuss further below, namely that the stress is determined by local conditions and can be computed from the local arrangement of atoms. If this assumption is valid, then we can compute the total force acting on the volume element by integrating the stress over its surface $\partial\mathcal{V}$:

$$\begin{aligned}\mathbf{F} &= -\int_{\partial\mathcal{V}} d\boldsymbol{\Sigma}\cdot\mathsf{T} \\ &= -\int_{\mathcal{V}} dV\,\boldsymbol{\nabla}\cdot\mathsf{T}\;,\end{aligned} \tag{10.30}$$

where we have invoked Gauss' theorem, and the minus sign is because $d\boldsymbol{\Sigma}$ points away from $\mathcal{V}$ instead of into it.

Box 10.2
Shear tensor in Spherical and Cylindrical Coordinates

Using our rules for forming the gradient of a vector we can derive a general expression for the shear tensor

$$\begin{aligned}\Sigma_{ij} &= \frac{1}{2}(\xi_{i;j}+\xi_{j;i})-\frac{1}{3}\delta_{ij}\xi_{k;k}\\ &= \frac{1}{2}(\xi_{i,j}+\xi_{j,i}+\Gamma_{ilj}\xi_l+\Gamma_{jli}\xi_l)-\frac{1}{3}\delta_{ij}(\xi_{k,k}+\Gamma_{klk}\xi_l)\ .\end{aligned} \tag{1}$$

Evaluating this *in cylindrical coordinates*, we obtain

$$\begin{aligned}\Sigma_{\varpi\varpi} &= \frac{2}{3}\frac{\partial\xi_\varpi}{\partial\varpi}-\frac{1}{3}\frac{\xi_\varpi}{\varpi}-\frac{1}{3\varpi}\frac{\partial\xi_\phi}{\partial\phi}-\frac{1}{3}\frac{\partial\xi_z}{\partial z}\\ \Sigma_{\phi\phi} &= \frac{2}{3\varpi}\frac{\partial\xi_\phi}{\partial\phi}+\frac{2}{3}\frac{\xi_\varpi}{\varpi}-\frac{1}{3}\frac{\partial\xi_\varpi}{\partial\varpi}-\frac{1}{3}\frac{\partial\xi_z}{\partial z}\\ \Sigma_{zz} &= \frac{2}{3}\frac{\partial\xi_z}{\partial z}-\frac{1}{3}\frac{\partial\xi_\varpi}{\partial\varpi}-\frac{1}{3}\frac{\xi_\varpi}{\varpi}-\frac{1}{3\varpi}\frac{\partial\xi_\phi}{\partial\phi}\\ \Sigma_{\phi z} &= \Sigma_{z\phi}=\frac{1}{2\varpi}\frac{\partial\xi_z}{\partial\phi}+\frac{1}{2}\frac{\partial\xi_\phi}{\partial z}\\ \Sigma_{z\varpi} &= \Sigma_{\varpi z}=\frac{1}{2}\frac{\partial\xi_\varpi}{\partial z}+\frac{1}{2}\frac{\partial\xi_z}{\partial\varpi}\\ \Sigma_{\varpi\phi} &= \Sigma_{\phi\varpi}=\frac{1}{2}\frac{\partial\xi_\phi}{\partial\varpi}-\frac{\xi_\phi}{2\varpi}+\frac{1}{2\varpi}\frac{\partial\xi_\varpi}{\partial\phi},\end{aligned} \tag{2}$$

Likewise, *in spherical coordinates*,

$$\begin{aligned}\Sigma_{rr} &= \frac{2}{3}\frac{\partial\xi_r}{\partial r}-\frac{2}{3r}\xi_r-\frac{\cot\theta}{3r}\xi_\theta-\frac{1}{3r}\frac{\partial\xi_\theta}{\partial\theta}-\frac{1}{3r\sin\theta}\frac{\partial\xi\phi}{\partial\phi}\\ \Sigma_{\theta\theta} &= \frac{2}{3r}\frac{\partial\xi_\theta}{\partial\phi}+\frac{\xi_r}{3r}-\frac{1}{3}\frac{\partial\xi_r}{\partial r}-\frac{\cot\theta\xi_\theta}{3r}-\frac{1}{3r\sin\theta}\frac{\partial\xi_\phi}{\partial\phi}\\ \Sigma_{\phi\phi} &= \frac{2}{3r\sin\theta}\frac{\partial\xi_\phi}{\partial\phi}+\frac{2\cot\theta\xi_\theta}{3r}+\frac{\xi_r}{3r}-\frac{1}{3}\frac{\partial\xi_r}{\partial r}-\frac{1}{3r}\frac{\partial\xi_\theta}{\partial\theta}\\ \Sigma_{\theta\phi} &= \Sigma_{\phi\theta}=\frac{1}{2r}\frac{\partial\xi_\phi}{\partial\theta}-\frac{\cot\theta\xi_\phi}{2r}+\frac{1}{2r\sin\theta}\frac{\partial\xi_\theta}{\partial\phi}\\ \Sigma_{\phi r} &= \Sigma_{r\phi}=\frac{1}{2r\sin\theta}\frac{\partial\xi_r}{\partial\phi}+\frac{1}{2}\frac{\partial\xi_\phi}{\partial r}-\frac{\xi_\phi}{2r}\\ \Sigma_{r\theta} &= \Sigma\theta r=\frac{1}{2}\frac{\partial\xi_\theta}{\partial r}-\frac{\xi_\theta}{2r}+\frac{1}{2r}\frac{\partial\xi_r}{\partial\theta}.\end{aligned} \tag{3}$$

This identity must be true for arbitrary volumes and so we can identify the *elastic force density* acting on an elastic solid, $\mathbf{f}$, by

$$\mathbf{f} = -\boldsymbol{\nabla} \cdot \mathbf{T} \,. \tag{10.31}$$

In elastostatic equilibrium, this force density must balance all other volume forces acting on the material, most commonly the gravitational force density so that

$$\mathbf{f} + \rho \mathbf{g} = 0 \tag{10.32}$$

where $\mathbf{g}$ is the acceleration due to gravity. (Again, there should be no confusion between the vector $\mathbf{g}$ and the metric tensor $\mathbf{g}$.) There are other possible external forces, some of which we shall encounter later in a fluid context, e.g. an electromagnetic force density. These can be added to Eq. (10.32).

The stress tensor is symmetric, as we saw in Chapter 1. It therefore has 6 independent components. Just as was the case with the strain, we can subtract off the trace of the stress tensor, to leave behind a symmetric, trace-free shear stress tensor. The trace part that we have subtracted is the isotropic part of the stress tensor and is known as the *pressure*. Fluids exert isotropic stresses, i.e. $\mathbf{T} = p\mathbf{g}$, where p is the pressure. They cannot exert shear stress when at rest. (As we shall discuss extensively in Part IV, moving fluids can exert a viscous shear stress.)

Now let us consider some examples of stresses:

(i) Atmospheric pressure is equal to the weight of the air in a column of unit area extending above the earth, and thus is roughly $p \sim \rho g H \sim 10^5$Pa, where $\rho \sim 1$ kg m^{-3} is the density of air, $g \sim 10$m s^{-2} is the acceleration of gravity at the earth's surface and $H \sim 10$km is the atmospheric scale height. The stress tensor is isotropic.

(ii) Suppose we hammer a nail into a block of wood. The hammer might weigh $m \sim 0.3$kg and be brought to rest from a speed of $v \sim 10$m s^{-1} in a distance of, say, $d \sim 3$mm. Then the average force exerted on the wood by the nail is $F \sim mv^2/d \sim 10^5$N. If this is applied over an effective area $A \sim 1$mm^2, then the magnitude of the typical stress in the wood is $\sim F/A \sim 10^{10}$Pa $\sim 10^5$atmosphere. There is a large shear component to the stress tensor, which is responsible for separating the fibers in the wood.

(iii) Neutron stars are as massive as the sun, $M \sim 2 \times 10^{30}$ kg, but have far smaller radii, $R \sim 10$km. Their surface gravities are therefore $g \sim GM/R^2 \sim 10^{12}$m s^{-2}, a billion times that encountered on earth. They have solid crusts of density $\rho \sim 10^{17}$kg m^{-3} that are about 1km thick. The magnitude of the stress will then be given following (i) by $\sim 10^{31}$Pa! This stress will be mainly hydrostatic, though as the material is solid, a significant fraction will be in the form of a shear stress.

(iv) Elementary particles interact through forces. Although, it makes no sense to describe this interaction using classical elasticity, it does make sense to make order of magnitude estimates of the associated stress. One promising fundamental model of these interactions involves *strings* which exert a tension, $T \sim \mu c^2 \sim g^2 c^4/8\pi G$, where μ is the mass per unit length, g is a coupling constant and G is Newton's constant of gravitation.

Numerically, $g^2 \sim 0.025$, $T \sim 10^{45}$Pa, and $\mu \sim 1$Megaton per fermi, where Megaton is not the TNT equivalent!

(v) As we shall discuss in Part VI, a popular cosmological theory called *inflation* postulates that the universe underwent a period of rapid, exponential expansion during its earliest epochs. This expansion was driven by the stress associated with a false vacuum. The action of this stress on the universe can be described quite adequately using a classical stress tensor. If the interaction energy is $E \sim 10^{15}$GeV, the supposed scale of grand unification, and the associated length scale is $l \sim \hbar c/E$, the magnitude of the stress is $\sim E/l^3 \sim 10^{97}(E/10^{15}\text{GeV})^4$Pa. The ultimate stress is presumably found associated with singularities, for example at the creation of the universe or inside a black hole. Here the characteristic energy is the Planck energy $(\hbar c^5/G)^{1/2} \sim 10^{19}$ GeV and the associated stress is $\sim 10^{113}$ Pa.

10.4.2 Elastic Moduli

Having introduced the stress and the strain tensors, we are now in a position to generalize Hooke's law by postulating a linear relationship between them. The most general linear equation relating two second rank tensors will involve a fourth rank tensor known as the *elastic modulus tensor*, $\mathbf{Y}$. In slot-naming index notation,

$$T_{ij} = Y_{ijkl}S_{kl} \tag{10.33}$$

Now, a general fourth rank tensor in three dimensions has $3^4 = 81$ independent components. Elasticity can get complicated! However, the situation need not be so dire. There are several symmetries that we can exploit. Let us look at the general case. As the stress tensor is symmetric, and only the symmetric part of the strain tensor creates stress (i.e., a solid-body rotation through some angle $\boldsymbol{\phi}$ produces no stress), $\mathbf{Y}$ is symmetric in its first pair of slots and also in its second pair: $Y_{ijkl} = Y_{jikl} = Y_{ijlk}$. There are therefore 6 independent components Y_{ijkl} for variable i, j and fixed k, l, and *vice versa*. In addition, as we show below, $\mathbf{Y}$ is symmetric under an interchange of its first and second pairs of slots: $Y_{ijkl} = Y_{klij}$. There are therefore $(6 \times 7)/2 = 21$ independent components in $\mathbf{Y}$. This is an improvement over 81. Furthermore, many substances, notably crystals, exhibit additional symmetries and this can reduce the number of independent components considerably.

The simplest, and in fact most common, case arises when the medium is *isotropic*. In other words, there are no preferred directions in the material. This occurs when the solid is polycrystalline or amorphous and completely disordered on a scale large compared with the atomic spacing, but small compared with the sample size.

If a body is isotropic, then its elastic properties must be describable by scalars. Now, the stress tensor $\mathbf{T}$, being symmetric, must have just two irreducible tensorial parts, $\mathbf{T}$ =(a scalar)$\mathbf{g}$+(a trace-free symmetric part); and the parts of the strain that can produce this stress are the scalar expansion Θ and the trace-free, symmetric shear $\mathbf{\Sigma}$, but not the rotation. The only linear, coordinate-independent relationship between this $\mathbf{T}$ and these θ and $\mathbf{\Sigma}$ involving solely scalars as proportionality quantities is

$$\mathbf{T} = -K\theta\mathbf{g} - 2\mu\mathbf{\Sigma}. \tag{10.34}$$

Here K is called the *bulk modulus* and μ the *shear modulus*, and the factor 2 is included for purely historical reasons.

It is commonly the case that these elastic moduli are constant, i.e. are independent of location in the medium, even though the medium is stressed in an inhomogeneous way. If so, we can immediately write down an expression for the elastic force density defined by Eq. (10.29).

$$\begin{aligned} \mathbf{f} = -\boldsymbol{\nabla}\cdot\mathbf{T} &= K\boldsymbol{\nabla}\Theta + 2\mu\boldsymbol{\nabla}\cdot\boldsymbol{\Sigma} \\ &= (K+\frac{1}{3}\mu)\boldsymbol{\nabla}(\boldsymbol{\nabla}\cdot\boldsymbol{\xi}) + \mu\nabla^2\boldsymbol{\xi}, \end{aligned} \tag{10.35}$$

where $\boldsymbol{\nabla}\cdot\boldsymbol{\Sigma}$ in index notation is $\Sigma_{ij;j}$. Extra terms must be added if we are dealing with less symmetric materials. However, the form of Eq. (10.35) will be sufficient for our needs.

If no other countervailing forces act in the interior of the material (e.g., if there is no gravitational force), and if, as in this chapter, the material is in a static, equilibrium state rather than vibrating dynamically, then this force density will have to vanish throughout the material's interior. This vanishing of $\mathbf{f} \equiv -\boldsymbol{\nabla}\cdot\mathbf{T}$ is just a fancy version of Newton's law "$\mathbf{F} = m\mathbf{a} = 0$ in static situations."

10.4.3 Energy of Deformation

When a wire of length L is stretched below its elastic limit by an amount $\Delta L = \xi$, the stored elastic energy is computable as the work done by the elastic force F, which is proportional to the extension, $F \propto \xi$:

$$\begin{aligned} W &= \int_0^\xi F(\xi')d\xi' \\ &= F(\xi)\xi/2 \propto \xi^2 \ , \end{aligned} \tag{10.36}$$

where ξ is the final extension.

The simplest way to generalize this formula is to imagine an elementary cube and compute the work done by the elastic stress. Let us orient a Cartesian coordinate system so that the faces are normal to the principal axes, labeled 1,2,3. Let the cube have sides L. Consider the stress acting on the face whose outward normal lies along the direction $\mathbf{e}_1$. The force the external medium exerts upon this face of the cube is a vector whose components are $-T_{i1}L^2$. Now suppose this surface has been displaced through a distance $\boldsymbol{\xi}$ as the stress has been applied. As the displacement is proportional to the applied force (i.e. $T_{i1} \propto \xi$), the total work performed by this force is $-T_{i1}L^2\xi_i/2$. The force acting on the opposite face of the cube acts in almost the opposite direction. To lowest order the work that it performs will cancel that done on the first face. However, expanding to first order in the separation, we find that the net work performed on these two faces will be

$$\Delta W_1 = -\frac{L^3}{2}\frac{\partial(\xi_i T_{i1})}{\partial x_1}. \tag{10.37}$$

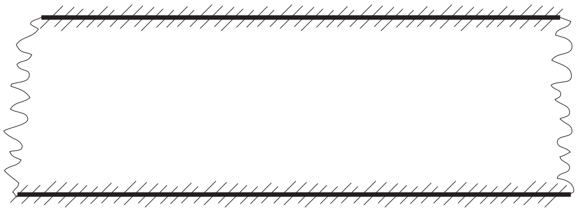

Fig. 10.3: Action of electromagnetic forces within a solid. If we compute the force acting on one side of the slice, the integral is dominated by interactions between atoms lying in the shaded area. The force is effectively a surface force rather than a volume force. In elastostatic equilibrium, the the forces acting on the two sides of the slice are effectively equal and opposite.

Identifying L^3 with the volume of the cube, and adding the contributions of the other two cubical faces, we find that the total net work per unit volume performed upon the cube is

$$\Delta w = -\frac{1}{2}(\xi_i T_{ij})_{;j}. \tag{10.38}$$

Does this equal the elastic energy stored in the lattice? The answer is "no", because we must also take account of the work done by the volume force **f** (cf. Eq. (10.31)) against the other forces that act on the cube (e.g. gravity) and keep it in equilibrium. If we assume that the displacement is made slowly, then these other stresses will exert a force per unit volume of $\boldsymbol{\nabla} \cdot \mathbf{T}$, which will do work per unit volume of $\xi_i T_{ij;j}/2$. The net increase in internal energy of the cube is, from the first law of thermodynamics, equal to the total work done. In other words,

$$\begin{aligned} U &= \frac{1}{2}[-(\xi_i T_{ij})_{;j} + \xi_i T_{ij;j}] \\ &= -\frac{1}{2}\xi_{i;j} T_{ij} \\ &= \frac{1}{2}K\Theta^2 + \mu \Sigma_{ij}\Sigma_{ij} \end{aligned} \tag{10.39}$$

where we have substituted Eq. (10.34). Note that this increase in internal energy is always positive if the elastic moduli are positive. This is clearly a necessary condition for matter to be stable to small perturbations.

For the more general, anisotropic case, expression (10.39) becomes

$$U = -\frac{1}{2}\xi_{i;j} Y_{ijkl} \xi_{k;l} \; . \tag{10.40}$$

The volume integral of this U can be used as an action from which to compute the stress, by varying the displacement. Since only the part of **Y** that is symmetric under interchange of the first and second pairs of slots contributes to U, then only that part can affect the action-principle-derived stress. Therefore, it must be that $Y_{ijkl} = Y_{klij}$. This is the symmetry we asserted earlier.

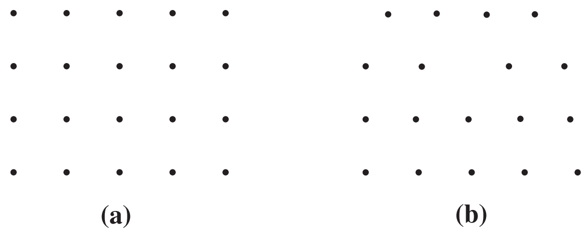

Fig. 10.4: a) A perfect crystal in which the atoms are organised in a perfectly repeating lattice can develop very large shear strains without yielding. b) Real materials contain dislocations which greatly reduce their rigidity. The simplest type of dislocation, shown here, is the *edge dislocation*. The dislocation will move and the crystal will undergo inelastic deformation when the stress is typically less than one per cent of the yield shear stress for a perfect crystal.

10.4.4 Molecular Origin of Elastic Stress

It is important to understand the microscopic origin of the elastic stress. Consider, an ionic solid in which singly ionized ions (e.g. sodium and chlorine) attract their nearest neighbours through their mutual Coulomb attraction and repel their next nearest neighbors and so on. Overall, there is a net attraction, which is balanced by the short range repulsion of the bound electrons. Now consider a thin slice of material of thickness intermediate between the inter-atomic spacing and the sample size, a few atomic spacings thick (Figure 10.3). If we calculate the force acting on the material in the slice exerted by external atoms on one side of the slice, we find that the sum converges very close to the boundary. Although the electrostatic force between individual atoms is long range, the material is electrically neutral and, when averaged over many atoms, the net electric force is of short range. We can therefore treat the net force acting on a region that is large enough to encompass many atoms, but much smaller than the size of the body under study, as a surface force governed by local conditions in the material. This is essential if we are to be able to write down a local, linear stress-strain relation $T_{ij} = Y_{ijkl}S_{kl}$. This need not have been the case and there are circumstances when a long range force develops. One example occurs with certain types of crystal (e.g. tourmaline) which develop internal, *piezoelectric* fields when strained.

Our treatment so far has implicitly made the assumption that matter is continuous on all scales and that derivatives are mathematically well-defined. Of course, this is not the case. In fact, we not only need to acknowledge the existence of atoms, we must use this fact to compute the elastic moduli.

We can estimate the elastic moduli in ionic or metallic materials by observing that if a crystal lattice were to be given a dimensionless strain of order unity, then the elastic stress would be of order the electrostatic force between adjacent ions divided by the area associated with each ion. If the lattice spacing is $a \sim 2$Å and the ions are singly charged, then $K, \mu \sim e^2/4\pi\epsilon_0 a^4 \sim 100$GPa. This is about a million atmospheres. Covalently bonded compounds are less tightly bound and have somewhat smaller elastic moduli. See Table 10.1.

It might be thought, on the basis of this argument that crystals can be subjected to strains of order unity before they attain their elastic limits. However, as explained above, most materials are only elastic for strains $\lesssim 10^{-3}$. The reason for this difference is that crystals are generally imperfect and are laced with *d*islocations. Relatively small stresses

Substance	K	μ	E	ν	c_L	c_T
	GPa	GPa	GPa		km s^{-1}	km s^{-1}
Steel	170	81	210	0.29	5.9	3.2
Copper	130	45	120	0.34	4.6	2.2
Glass	47	28	70	0.25	5.8	3.3
Rubber	10	0.0007	0.002	0.50	1.0	0.03

Table 10.1: Bulk, Shear and Young's moduli and Poisson's ratio for a range of materials. The final two columns quote the longitudinal and transverse sound speeds defined in the following chapter.

suffice for the dislocations to move through the solid and for the crystal thereby to undergo permanent deformation (Figure 10.4).

10.4.5 Young's Modulus and Poisson's Ratio for Isotropic Material

Consider a slender strut of square cross section lying along the $\mathbf{e}_z$ direction of a Cartesian coordinate system. Subject the strut to a compressive force applied normally and uniformly at its ends. (It could just as easily be a wire under extension.) Let its sides be free to expand transversely, so that no force acts on its sides, $dF_i = T_{ij} d\Sigma_j = 0$. As the strut is slender, vanishing of the dF_i at its sides implies to high accuracy that the stress components T_{ix} and T_{iy} will vanish throughout the interior; otherwise there would be a large force density inside the strut. Applying Eqs. (10.34) and (10.7) to relate the strain to the applied stress, we then obtain

$$\begin{aligned}
T_{xx} = T_{yy} &= -K\Theta - 2\mu\Sigma_{xx} = 0 \, , \\
T_{yz} &= -2\mu\Sigma_{yz} = 0 \, , \\
T_{xz} &= -2\mu\Sigma_{xz} = 0 \, , \\
T_{xy} &= -2\mu\Sigma_{xy} = 0 \, , \\
T_{zz} &= -K\Theta - 2\mu\Sigma_{zz} \, .
\end{aligned} \tag{10.41}$$

We have appealed to obvious symmetries. Solving these equations, we obtain for the measured longitudinal strain, $\xi_{z,z}$ [cf. Eqs. (10.2) and (10.7)]

$$\begin{aligned}
\xi_{z,z} &= \Sigma_{zz} + \frac{1}{3}\Theta \\
&= \frac{(3K+\mu)}{3\mu}\Theta.
\end{aligned} \tag{10.42}$$

where we have used the first of Eq. (10.41) and the fact that the trace of the shear tensor vanishes so that $\Sigma_{zz} = -2\Sigma_{xx}$. *Young's modulus* E is defined to be the ratio of the applied stress $(-T_{zz})$ to the longitudinal strain,

$$E = \frac{-T_{zz}}{\xi_{z,z}} = \frac{9\mu K}{3K+\mu} \tag{10.43}$$

where we have substituted the last of Eqs. (10.41) and Eq. (10.42).

It is also conventional to introduce *Poisson's ratio*, ν, which is defined to be minus the ratio of the lateral strain to the longitudinal strain during a deformation of this type in which the transverse motion is unconstrained. It can be expressed as a ratio of elastic moduli as follows.

$$\begin{aligned}\nu &= -\frac{\xi_{x,x}}{\xi_{z,z}} \\ &= -\frac{\Sigma_{xx} + \frac{1}{3}\Theta}{\Sigma_{zz} + \frac{1}{3}\Theta} \\ &= \frac{3K - 2\mu}{2(3K + \mu)}.\end{aligned} \tag{10.44}$$

We can invert these two equations to obtain

$$\begin{aligned}K &= \frac{E}{3(1 - 2\nu)} \\ \mu &= \frac{E}{2(1 + \nu)}.\end{aligned} \tag{10.45}$$

We have already remarked that mechanical stability of a solid requires that $K, \mu > 0$. Using Eq. (10.45), we observe that this imposes a restriction on Poisson's ratio, namely that $-1 < \nu < 1/2$. For metals, Poisson's ratio is typically 1/3 and the shear modulus is roughly half the bulk modulus. For a substance that is easily sheared but not easily compressed, like rubber, the bulk modulus is relatively high and $\nu \simeq 1/2$ (cf. Table 10.1.) For some exotic materials, Poison's ratio can be negative (cf. Yeganeh-Haeri *et al* 1992).

Although we derived them for a square strut under compression, our expressions for Young's modulus and Poisson's ratio are quite general. To see this, observe that the derivation would be unaffected if we combined many parallel, square fibers together. All that is necessary is that the transverse motion be free so that the only applied force is normal to one end.

****

EXERCISES

Exercise 10.3 *Problem: Order of Magnitude Estimates*

(i) What length of steel wire can hang vertically without breaking?

(ii) What is the maximum size of a non-spherical asteroid?

(iii) Can a helium balloon lift the tank used to transport the helium?

Exercise 10.4 *Example: Fracture of a Pipe*
As an example of a very practical application of the theory of elasticity, calculate the maximum pressure inside a hollow, cylindrical pipe allowed before there is danger of fracture.

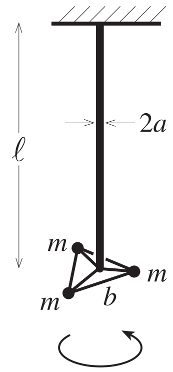

Fig. 10.5: Torsion Pendulum

(i) Use the connection coefficients from Eqs. (10.20) and (10.21) to verify the expressions given in Box 10.4 for the components of the shear tensor in cylindrical coordinates.

(ii) Now consider a cylindrical pipe of inner radius R_1 and outer radius R_2 and fixed length L that transports fluid at pressure p much larger than the exterior pressure which can be approximated as zero. It is made out of material with $E = 100$GPa and $\nu = 0.3$. Show that the displacement $\boldsymbol{\xi}$ of the material in the pipe is purely radial and use Eq. (10.35) to show that the expansion Θ of the material is a constant, i.e. is independent of radius r. Hence show that the radial displacement can be written in the form

$$\xi_r = Ar + \frac{B}{r} \ .$$

Obtain expressions for the non-vanishing components of the strain tensor.

(iii) Next derive expressions for the components of the stress tensor in cylindrical coordinates. Impose pressure boundary conditions at R_1, R_2 to identify A, B. Hence show that there is a force inside the pipe walls, parallel to its axis of magnitude $2\pi\nu p R_1^2$.

(iv) Measure the magnitude of the strain by the skew angle $\phi = 2(\xi_{\phi,\phi} - \xi_{r,r})$ and require that this be smaller than 10^{-4} for safety. Hence, estimate the minimum wall thickness needed if a $R_2 = 30$mm radius pipe is required to transport oil at 10 atmospheres.

Exercise 10.5 *Practice: Torsion pendulum*
A torsion pendulum is a very useful tool for performing the classical Eötvös experiment and for seeking evidence for hypothetical *fifth* (not to mention *sixth*) forces. It would be advantageous to design a torsional pendulum with a one day period (Figure 10.5). This exercise is designed to see if this is possible. The pendulum consists of a thin cylindrical wire of length l and radius a. At the bottom of the wire are suspended three masses (one gold, two aluminum) at the corners of an equilateral triangle at a distance b from the wire.

(i) Show that the longitudinal strain is

$$\epsilon = \frac{mg}{\pi a^2 E}$$

(ii) Show that the assembly undergoes torsional oscillations with period

$$P = 2\pi \left(\frac{\ell}{g}\right)^{1/2} \left(\frac{2bE\epsilon}{a\mu}\right)^{1/2}$$

(iii) Do you think you could design an experiment to attain the goal of a one day period?

****

10.5 Thermoelastic Noise in Gravitational-Wave Detectors

Foundations

We turn now to our first application of elasticity theory – one that illustrates a number of concepts that we have developed in this chapter, as well as some from previous chapters. This application is the computation of *theromelastic noise* in second-generation gravitational-wave detectors such as LIGO-II. Our analysis is based on recent research by Braginsky, Gorodetsky and Vyatchanin (1999); see also Liu and Thorne (2000).

We discussed laser interferometer gravitational-wave detectors in Sec. 8.5 (see especially Fig. 8.11). Recall that in such a detector, a gravitational wave moves four test-mass mirrors relative to each other, and laser interferometry is used to monitor the resulting oscillatory changes in the mirror separations. As we discussed in Sec. 5.6, the separations actually measured are the differences in the mirrors' generalized coordinates q, each of which is the longitudinal position ξ_z of the test mass's mirrored front face, weighted by the laser beam's Gaussian-shaped intensity distribution and averaged over the mirror's face:

$$q = \int \frac{e^{-\varpi^2/\varpi_o^2}}{\pi\varpi_o^2} \xi_z(\varpi, \phi) d\phi d\varpi \qquad (10.46)$$

[Eq. (5.107) with a change of notation]. Here (ϖ, ϕ, z) are cylindrical coordinates with the axis $\varpi = 0$ along the center of the laser beam, $\varpi_o \sim 4$ cm is the radius at which the light's intensity has dropped by a factor $1/e$, and $\xi_z(\varpi, \phi)$ is the longitudinal displacement of the mirror face. The gravitational-wave signal is the difference of mirror positions divided by the interferometer arm length $L = 4$ km: $h(t) = \{[q_1(t) - q_2(t)] - [q_3(t) - q_4(t)]\}/L$, where the subscripts label the four mirrors. The thermoelastic noise is uncorrelated between the four test masses and, because the test masses and the beam spots on them are identical, it is the same in all four test masses—which means that the spectral densities of their noises add incoherently, giving

$$S_h(f) = \frac{4S_q(f)}{L^2} \, . \qquad (10.47)$$

Here $S_q(f)$ is the spectral density of the fluctuations of the generalized coordinate q of any one of the test masses.

The thermoelastic noise is a variant of *thermal noise*; it arises when fluctuations of the thermal energy distribution inside a test mass randomly cause a slight increase (or decrease) in the test-mass temperature near the laser beam spot, and a corresponding thermal expansion (or contraction) of the test-mass material near the beam spot. This random expansion (or contraction) entails a displacement ξ_z of the test-mass surface and a corresponding random change of the generalized coordinate q.

In Ex. 10.6 we use the fluctuation-dissipation theorem (Sec. 5.6) to derive the following prescription for computing the spectral density $S_q(f)$ of these random thermoelastic fluctuations of q. Our prescription is expressed in terms of a thought experiment: Imagine applying a static, normal (z-directed) force F_o to the face of the test mass at the location of the beam spot, with the force distributed spatially with the same Gaussian profile as q so the applied stress is

$$T_{zz}^{\rm applied} = \frac{e^{-\varpi^2/\varpi_o^2}}{\pi\varpi_o^2} F_o \; . \tag{10.48}$$

This applied stress induces a strain distribution $\mathbf{S}$ inside the test mass, and that strain includes an expansion $\Theta(\varpi, \phi, z)$. The analysis in Ex. 10.6 shows that the spectral density of thermoelastic noise is expressible as follows in terms of an integral over the squared gradient of this expansion:

$$S_q(f) = \frac{2\kappa_{\rm th} E^2 \alpha^2 k T^2}{(1-2\nu)^2 C_V^2 \rho^2 F_o^2 (2\pi f)^2} \left\langle \int (\boldsymbol{\nabla}\Theta)^2 \varpi d\phi d\varpi dz \right\rangle \; . \tag{10.49}$$

Here $\kappa_{\rm th}$ is the coefficient of thermal conductivity (Sec. 2.8), E is Young's modulus, ν is the Poisson ratio, α is the coefficient of linear thermal expansion (fractional change of length induced by a unit change of temperature), T is temperature, C_V is the specific heat per unit mass at constant volume, ρ is the density, and f is the frequency at which the noise is being evaluated.

The computation of the thermoelastic noise, thus, boils down to computing the distribution $\Theta(\varpi, \phi, z, t)$ of expansion induced by the applied stress (10.48), and then evaluating the integral in Eq. (10.49). The computation is made easier by the fact that Θ and $\boldsymbol{\nabla}\Theta$ are concentrated in a region of size $\sim \varpi_o \sim 40$ mm, which is small compared to the test-mass radius and length ($\sim$).14 m), so in our computation we can idealize the test mass as having infinite radius and length (i.e., as being an "infinite half space").[2]

Equations of Elasticity in Cylindrical Coordinates, and their Solution

Because the applied stress is cylindrical, the induced strain and expansion will also be cylindrical, and are thus computed most easily using cylindrical coordinates.

The expansion Θ and the components of the shear $\boldsymbol{\Sigma}$ are given in terms of the components ξ_ϖ and ξ_z by Eqs. (10.26) and (2) of Box 10.3, with $\xi_\phi = 0$ and with vanishing dependence on ϕ. Inserting these Θ and $\boldsymbol{\Sigma}$ into Eq. (10.34) for the test mass's internal stress $\mathbf{T}$, and computing the divergence of this stress in cylindrical coordinates with the aid of the connection coefficients (10.20), and expressing the bulk and shear moduli in terms of

[2]Finiteness of the test mass turns out to increase $S_q(f)$ by about 20 per cent (Liu and Thorne, 2000).

the Young's modulus and Poisson ratio [Eq. (10.45)], we obtain the following equations for stress balance [Ex. 10.7]:

$$
\begin{aligned}
T_{\varpi j;j} &= \frac{-E}{2(1+\nu)(1-2\nu)}\left[2(1-\nu)\left(\frac{\partial^2\xi_\varpi}{\partial\varpi^2}+\frac{1}{\varpi}\frac{\partial\xi_\varpi}{\partial\varpi}-\frac{\xi_\varpi}{\varpi^2}\right)\right. \\
&\qquad\left. +(1-2\nu)\frac{\partial^2\xi_\varpi}{\partial z^2}+\frac{\partial^2\xi_z}{\partial z\partial\varpi}\right]=0\ , \\
T_{zj;j} &= \frac{-E}{2(1+\nu)(1-2\nu)}\left[(1-2\nu)\left(\frac{\partial^2\xi_z}{\partial\varpi^2}+\frac{1}{\varpi}\frac{\partial\xi_z}{\partial\varpi}\right)\right. \\
&\qquad\left. +2(1-\nu)\frac{\partial^2\xi_z}{\partial z^2}+\frac{\partial^2\xi_\varpi}{\partial z\partial\varpi}+\frac{1}{\varpi}\frac{\partial\xi_\varpi}{\partial z}\right]=0\ .
\end{aligned}
\tag{10.50}
$$

These are two coupled, linear, second-order differential equations for the two unknown components of the displacement vector. As with the analogous equations of electrostatics and magnetostatics, these can be solved by separation of variables. We seek a solution that dies out at large z and ϖ. The general variables-separated solution of this sort is

$$
\begin{aligned}
\xi_\varpi &= \int_0^\infty \left[\alpha(k)-(2-2\nu-kz)\beta(k)\right]e^{-kz}J_1(k\varpi)k\,dk\ , \\
\xi_z &= \int_0^\infty \left[\alpha(k)+(1-2\nu+kz)\beta(k)\right]e^{-kz}J_0(k\varpi)\,dk\ ,
\end{aligned}
\tag{10.51}
$$

where J_0 and J_1 are Bessel functions of order 0 and 1.

Boundary Conditions

The functions $\alpha(k)$ and $\beta(k)$ are determined by boundary conditions on the face of the test mass: The force per unit area exerted across the face by the strained test-mass material, T_{zj} at $z=0$ with $j=\{\varpi,\phi,z\}$, must be balanced by the applied force per unit area, $T_{zj}^{\rm applied}$ [Eq. (10.48)]. The (shear) forces in the ϕ direction, $T_{z\phi}$ and $T_{z\phi}^{\rm applied}$, vanish because of cylindrical symmetry and thus provide no useful boundary condition. The (shear) force in the ϖ direction, which must vanish since $T_{z\varpi}^{\rm applied}=0$, is given by [cf. Eq. (2) in Box 10.3]

$$
T_{z\varpi}(z=0) = -2\mu\Sigma_{z\varpi} = -\frac{\partial\xi_z}{\partial\varpi}-\frac{\partial\xi_\varpi}{\partial z} = -2\mu\int_0^\infty \left[\beta(k)-\alpha(k)\right]J_1(kz)k\,dk = 0\ , \tag{10.52}
$$

which implies that $\beta(k)=\alpha(k)$. The (normal) force in the z direction, which must balance the applied normal force, is $T_{zz}=-K\Theta-2\mu\Sigma_{zz}$; using Eq. (2) in Box 10.3 and Eqs. (10.51), this reduces to

$$
T_{zz}(z=0) = -2\mu\int_0^\infty \alpha(k)J_0(k\varpi)k\,dk = T_{zz}^{\rm applied} = \frac{e^{-\varpi^2/\varpi_o^2}}{\pi\varpi_o^2}F_o\cos(2\pi f t)\ , \tag{10.53}
$$

which can be inverted[3] to give

$$
\alpha(k)=\beta(k)=-\frac{1}{4\pi\mu}e^{-k^2\varpi_o^2/4}F_o\cos(2\pi f t)\ . \tag{10.54}
$$

[3]The inversion and the subsequent evaluation of the integral of $(\boldsymbol{\nabla}\Theta)^2$ are aided by the following expressions for the Dirac delta function: $\delta(k-k')=k\int_0^\infty J_0(k\varpi)J_0(k'\varpi)\varpi d\varpi = k\int_0^\infty J_1(k\varpi)J_1(k'\varpi)\varpi d\varpi$.

Inserting this into the Eqs. (10.51) for the displacement, and then evaluating the expansion [Eq. (1) of Box 10.3], we obtain

$$\Theta = -4\nu \int_0^\infty \alpha(k) e^{-kz} J_0(k\varpi) k dk \ . \tag{10.55}$$

It is now straightforward to compute the gradient of this expansion, square and integrate to get the spectral density $S_q(f)$ [Eq. (10.49)]. That result, when inserted into Eq. (10.47) gives, for the gravitational-wave noise,

$$S_h(f) = \frac{32(1+\nu)^2 \kappa_{\rm th} \alpha^2 k T^2}{\sqrt{2\pi} C_V^2 \rho^2 \varpi_o^3 (2\pi f)^2} \ . \tag{10.56}$$

It is planned to make the test masses from sapphire, for which $\nu = 0.29$, $\kappa_{\rm th} = 40$ W m^{-1} K^{-1}, $\alpha = 5.0 \times 10^{-6}$ K^{-1}, $C_V = 790$ J kg^{-1} K^{-1}, $\rho = 4000$ kg m^{-3}. Inserting these into Eq. (10.56), along with the interferometer arm length $L = 4$ km, a laser-beam radius $\varpi_o = 40$ mm, and room temperature $T = 300$ K, we obtain the following result for the thermoelastic gravity-wave noise in a bandwidth equal to frequency:

$$\sqrt{f S_h(f)} = 2.6 \times 10^{-23} \sqrt{\frac{100\text{Hz}}{f}} \ . \tag{10.57}$$

We shall explore the consequences of this noise for gravitational-wave detection in Part VI.

****

EXERCISES

Exercise 10.6 *Derivation and Example: Thermoelastic Noise*
Derive Eq. (10.49) for the thermoelastic noise in a gravitational-wave test mass by the following steps: First, read the discussion of the fluctuation-dissipation theorem in Sec. 5.6, and then read Ex. 5.7, which is the starting point for the derivation. Our $S_q(f)$ is given by Eq. (5.150). The key unknown quantity in this equation is the dissipation rate $W_{\rm diss}$ associated with a sinusoidally oscillating applied stress [Eq. (10.48), multiplied by $\cos(2\pi f t)$].

a. There are three important time scales in this problem: (i) the oscillation period of the applied stress $\tau_{\rm applied} = 1/f \sim 0.01$ s, (ii) the time $\tau_{\rm sound}$ for sound waves to travel across the test mass (a distance $\sim$ 14 cm; the sound speed, as we shall see in Chap. 11, is roughly $\sqrt{E/\rho}$), and (iii) the time $\tau_{\rm heat}$ for diffusive heat conductivity to substantially change the temperature distribution inside the test mass (cf. the discussion of heat conductivity in Sec. 2.8). Estimate, roughly, $\tau_{\rm sound}$ and $\tau_{\rm heat}$, and thereby show that $\tau_{\rm sound} \ll \tau_{\rm applied} \ll \tau_{\rm heat}$. Explain why this means that in evaluating $W_{\rm diss}$, we can (i) treat the test-mass strain as being produced quasistatically (i.e., we can ignore the inertia of the test-mass material), and (ii) we can treat the expansion of the test-mass material adiabatically (i.e., ignore the effects of heat flow when computing the temperature distribution in the test mass).

b. Show that, when the test-mass material adiabatically expands by an amount $\Delta V/V = \Theta$, its temperature goes down by

$$\delta T = \frac{-\alpha E T}{C_V \rho (1-2\nu)} \Theta \; . \tag{10.58}$$

[For a textbook derivation of this, see Sec. 6 of Landau and Lifshitz (1970). In that section a clean distinction is made between the bulk modulus K for expansions at constant temperature and that $K_{\rm ad}$ for adiabatic expansion. For most materials, these bulk moduli are nearly the same; for example, for sapphire they differ by only ~ 1 part in 10^5 [cf. Eqs. (6.7), (6.8) of Landau and Lifshitz (1970) and the numbers for sapphire at the end of the above Section; and note the difference of notation: α of this paper is $1/3$ that of Landau and Lifshitz, and $C_V \rho$ of this paper is C_V of Landau and Lifshitz].

c. The inhomogeneity of the expansion Θ causes the temperature perturbation δT to be inhomogeneous, and that inhomogeneity produces a heat flux $\mathbf{q} = -\kappa_{\rm th} \boldsymbol{\nabla} \delta T$. Whenever an amount Q of heat flows from a region of high temperature T to one of slightly lower temperature $T - dT$, there is an increase of entropy, $dS = Q/(T-dT) - Q/T = Q dT/T^2$. Show that for our situation, the resulting rate of entropy increase per unit volume is

$$\frac{dS}{dV dt} = \frac{-\mathbf{q} \cdot \boldsymbol{\nabla} \delta T}{T^2} = \frac{\kappa_{\rm th} \cdot (\boldsymbol{\nabla} \delta T)^2}{T^2} \; . \tag{10.59}$$

(We shall rederive this fundamental result from a different viewpoint in Part IV.)

d. This entropy increase entails a creation of new thermal energy at a rate per unit volume $dE_{\rm th}/dV dt = T dS/dV dt$. Since, for our thought experiment with temporally oscillating applied stress, this new thermal energy must come from the oscillating elastic energy, the rate of dissipation of elastic energy must be

$$W_{\rm diss} = \int \kappa_{\rm th} (\boldsymbol{\nabla} \delta T)^2 T dV \; . \tag{10.60}$$

By combining with Eq. (10.58), inserting into Eq. (5.150) and averaging over the period $\tau_{\rm applied}$ of the applied force, derive Eq. (10.49) for $S_q(f)$. Explain why, in this equation, we can treat the applied force as static rather than oscillatory, which is what we did in the text.

Exercise 10.7 *Derivation and Practice: Evaluation of Divergence of Stress Tensor*
Following the procedure outlined in the text, derive Eqs. (10.50) for the divergence of the stress tensor for a cylindrically symmetric system.

****

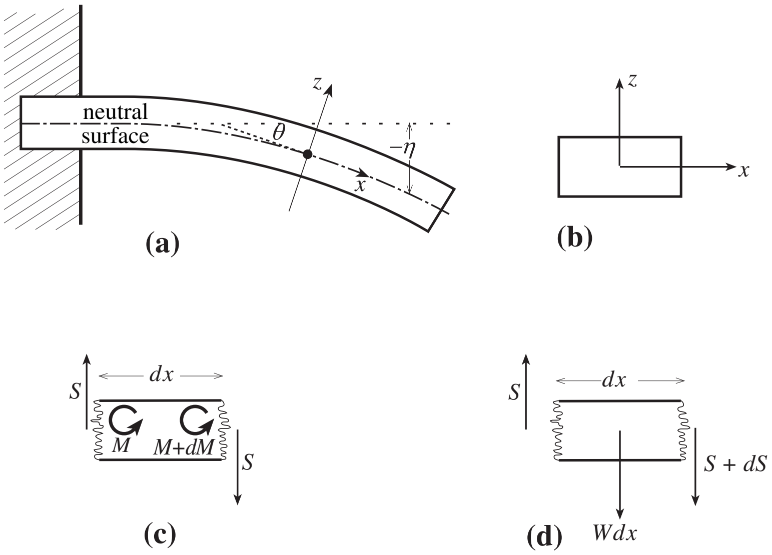

Fig. 10.6: Bending of a cantilever. a) A beam is held rigidly at one end and extends horizontally with the other end free. We introduce an orthonormal coordinate system (x, y, z) with $\mathbf{e}_x$ extending along the beam. We only consider small departures from equilibrium. The bottom of the beam will be compressed, the upper portion extended. There is therefore a neutral surface on which the strain vanishes. b) The beam shown here has rectangular cross section with horizontal width w, vertical thickness t and length ℓ. c) The bending torque M must be balanced by the torque exerted by the vertical shearing force S. d) S must vary along the beam so as to support the beam's weight per unit length, W.

10.6 Bending of Beams - Cantilever Bridges

One common method of bridge construction uses cantilevers. (A famous historical example is the old bridge over the Firth of Forth in Scotland that was completed in 1890 with a main span of half a km.) The principle used is to attach two independent beams to the two shores and allow them to meet in the middle. (In practice the beams are usually supported at the shores on piers and strengthened along their lengths with trusses.)

Let us make a simple model of a cantilever (Figure 10.6). Consider a beam clamped rigidly at one end, with length ℓ, horizontal width w and vertical thickness t. Introduce local cartesian coordinates with $\mathbf{e}_x$ extending along the beam and $\mathbf{e}_z$ extending vertically upward. Imagine the beam extending horizontally in the absence of gravity. Now let it sag under its own weight so that each element is dispaced through a small distance $\boldsymbol{\xi}(\mathbf{x})$. Clearly the upper part of the beam will be stretched while the lower part will be compressed. There must therefore be a *neutral surface* where the strain measured along the beam vanishes. This neutral surface must itself be curved downward. Let its displacement from the horizontal plane that it occupied before sagging be $\eta(x)(< 0)$, and let a plane tangent to the neutral surface make an angle $\theta(x)$ with the horizontal. The longitudinal strain is then given to first order in small quantities by

$$\xi_{x,x} = -z\frac{d\theta}{dx} \simeq -z\frac{d^2\eta}{dx^2} \tag{10.61}$$

Once again, we can regard the beam as being composed of a bundle of long parallel fibres, stretched along their length and free to contract transversely as with the strut considered above. The longitudinal stress is therefore

$$T_{xx} = -E\xi_{x,x} = Ez\frac{d^2\eta}{dx^2}. \tag{10.62}$$

We can now compute the horizontal force density, which must vanish in elastostatic equilibrium

$$f_x = -T_{xx,x} - T_{xz,z} = -Ez\frac{d^3\eta}{dx^3} - T_{xz,z} = 0. \tag{10.63}$$

Now multiply Eq. (10.63) by z and integrate over z to remove the derivative. We obtain

$$\frac{Et^3}{12}\frac{d^3\eta}{dx^3} = \int_{-t/2}^{t/2} dzT_{xz}. \tag{10.64}$$

(We have integrated the final term by parts and assumed that the shear stress vanishes on the upper and lower surface.) The next step is to use the symmetry of the stress tensor, $T_{xz} = T_{zx}$ to compute the total vertical *shearing force* $S(x)$ acting in the beam

$$S = w\int_{-t/2}^{t/2} dzT_{zx} = D\frac{d^3\eta}{dx^3}. \tag{10.65}$$

The quantity

$$D = E\int dydzz^2 = Ewt^3/12 \tag{10.66}$$

is called the *flexural rigidity.*

At this point, we can gain some insight into what is happening by defining the torque exerted by the longitudinal stress T_{xx}, called the *bending torque*, that one segment of the beam exerts on the neighboring segment.

$$M = \int dydzzT_{xx}. \tag{10.67}$$

Eq. (10.65) then has the form $dM - Sdx = 0$, which means that there is torque balance along the beam.

The final step is to recognize that the shearing force must support the weight of the beam.

$$\frac{dS}{dx} = -W\ , \tag{10.68}$$

where W is the weight per unit length of the beam. Combining with Eq. (10.65), we obtain a fourth order differential equation

$$\frac{d^4\eta}{dx^4} = -\frac{W}{D} \tag{10.69}$$

Fourth order differential equations are characteristic of elasticity. Eq. (10.69) can be solve subject to four appropriate boundary conditions.

However, before we do this, note that for a beam of a fixed length, the deflection η is inversely proportional to the flexural rigidity. Let us give a simple example of this scaling. Floors are conventionally supported by wooden *joists* of 2" by 6" lumber with the 6" side vertical. Suppose an inept carpenter installed the joists with the 6" side horizontal. The flexural rigidity of the joist would be reduced by a factor 9 and the center of the floor would be expected to sag 9 times as much as if the joists had been properly installed – a potentially catastrophic error.

Also, before considering the solution of this equation, we should emphasize the approximations that we have made. Firstly, we have assumed that the sag is small compared with the length of the beam in making the small angle approximation in Eq. (10.61). This will usually be the case. Secondly, by dealing with global forces rather than solving for the complete local stress tensor field, we have ignored the effect of some components of the stress tensor. In particular, in evaluating the bending torque we have ignored the effect of the T_{zx} component of the stress tensor. This is $O(t/\ell)T_{xx}$ and so our equations can only be accurate for fairly slender beams. Thirdly, the extension above the neutral surface and the compression below the neutral surface lead to changes in the shape of the beam. The fractional error here is of order the longitudinal shear, which is small for real materials.

We solve Eq. (10.69) using as a fourth order polynomial with four unknown constants to be set from the boundary conditions. In this problem, the beam must be held horizontally at the fixed end so that $\eta(0) = \eta'(0) = 0$. At the free end, the bending torque and the shearing force must vanish, so that $\eta''(\ell) = \eta'''(\ell) = 0$. The end result of imposing these conditions is that the end of the beam sags by

$$-\eta(\ell) = \frac{W\ell^4}{8D} \tag{10.70}$$

Problems in which the beam rests on supports rather than is clamped can be solved in a similar manner.

Now suppose that we have a cantilever bridge of constant vertical thickness t and total span $L \sim$100m made of material with density $\rho \sim 8 \times 10^3$kg m^{-3} (e.g. reinforced concrete) and Young's modulus $E \sim 100$GPa. Suppose further that we want the center of the bridge to sag by no more than $\eta \sim 1$m. According to Eq. (10.70), the thickness of the beam must satisfy

$$t \gtrsim \left(\frac{3\rho g L^4}{32 E\eta}\right)^{1/2} \sim 2\text{m} \tag{10.71}$$

This estimate makes no allowance for all the extra strengthening and support present in real structures and so it is an overestimate.

****

EXERCISES

Exercise 10.8 *Derivation: Sag in a cantilever*

(i) Verify Eq. (10.70) for the sag in a horizontal beam clamped at one end and allowed to hang freely at the other end.

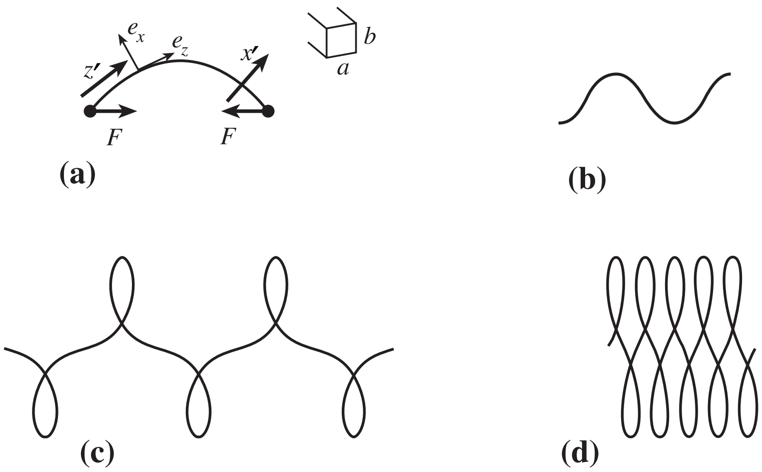

Fig. 10.7: Elastica. a) A bent wire is in elastostatic equilibrium under the action of equal and opposite forces applied at its two ends. z' measures distance along the neutral surface; x' measures horizontal distance in the perpendicular direction. b), c), d) Examples of the resulting shapes.

(ii) Now consider a similar beam with constant cross section and loaded with weights so that the total weight per unit length is $W(x)$. Give a Green's function for the sag of the free end in terms of an integral over $W(x)$.

Exercise 10.9 *Example: Elastica*

Consider a slender wire of rectangular cross section resting on a horizontal surface, with horizontal thickness a and vertical thickness b. Let the wire be bent in the horizontal $(x-z)$ plane as a result of forces that act at its ends. The various shapes that it can assume are called *elastica* and were first computed by Euler in 1744. The differential equation that governs the shape of the wire is similar to that derived for the cantilever, Eq. (10.69) with the simplification that the wire's weight does not enter the problem. Now the total force $\mathbf{F}$ applied externally at one end must be balanced by an equal and opposite force $-\mathbf{F}$ applied at the other end.

It is convenient to introduce curvilinear coordinates with coordinate z' measuring distance along the neutral surface $y' = y$ measured vertically, and x' measured orthogonal to z' in the x-z plane. The unit vectors along the x', y', and z' directions we shall denote by $\mathbf{e}_x$, $\mathbf{e}_y$, $\mathbf{e}_z$ (Figure 10.7). Let $\theta(z')$ be the angle between $\mathbf{e}_z$ and $\mathbf{F}$. $\theta(z')$ is determined by force and torque balance.

(i) Show that

$$
\begin{aligned}
F\cos\theta &= \int T_{z'z'}dx'dy' \,, \\
F\sin\theta &= \int T_{x'z'}dx'dy' \\
&= \frac{dM}{dz'} \,,
\end{aligned}
$$

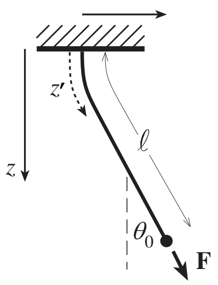

Fig. 10.8: Foucault Pendulum

where the bending torque, $M = \int x' T_{z'z'} dx' dy'$, satisfies

$$M = -D\frac{d\theta}{dz'} \ .$$

Hence show that

$$\frac{d^2\theta}{dz'^2} = -\frac{F\sin\theta}{D} \ ,$$

where D is the flexural rigidity [cf. Eq. (10.66)]. This is the same equation as that describing the motion of a simple pendulum!

(ii) Find one non-trivial solution of this equation either analytically using elliptic integrals or numerically.

(iii) Solve for the shape adopted by the wire corresponding to your solution in (ii). It is necessary to express the curvature of the wire, $d\theta/dz$ in terms of our original coordinates, x, z using the differential equation

$$\frac{d^2z}{dx^2}\left[1 + \left(\frac{dz}{dx}\right)^2\right]^{-3/2} = \frac{d\theta}{dz'} \ .$$

Again either analytic or numerical solutions can be sought, a Runge-Kutta scheme being particularly useful for the latter.

(iv) Obtain a uniform piece of wire and adjust the force $\mathbf{F}$ to compare your answer with experiment.

Exercise 10.10 *Example: Foucault Pendulum*
In the design of a Foucault pendulum for measuring the earth's general relativistic "gravitomagnetic field" (discussed further in Part VI), it is crucial that the pendulum's restoring force be isotropic. The answer to the previous question can be adapted to model the effect of anisotropy in the wire on the period.

(i) Consider a pendulum of mass m and length ℓ suspended as shown in Figure 10.8 by a rectangular wire with sides a and b along the x and y directions. Explain why the force that the wire exerts on the mass is $-\mathbf{F} = -(mg_e \cos\theta_o + m\ell\dot{\theta}_o^2)\mathbf{e}_{z'}$, where $\dot{\theta}_o$ is the time derivative of θ_o due to the swinging of the pendulum and in the second term we have assumed that the wire is long compared to its region of bend. Express the second term in terms of the amplitude of swing $\theta_o^{\rm max}$, and show that for small amplitudes $\theta_o^{\rm max} \ll 1$, $\mathbf{F} \simeq mg_e\mathbf{e}_{z'}$. Use this approximation in the subsequent parts

(ii) Assuming $\theta \ll 1$, show that

$$\theta(z') = \theta_o[1 - e^{-z'/\lambda}] ,$$

where

$$\lambda = \frac{a}{(12\epsilon)^{1/2}} ,$$

$\epsilon = \xi_{z',z'}$ is the longitudinal strain in the wire, and a is the wire's thickness along its direction of swing (the x direction). Note that the bending of the wire is concentrated near the support, so this is where dissipation will be most important.

(iii) Hence show that the shape of the wire is given in terms of cartesian coordinates by

$$x = [z - \lambda(1 - e^{-z/\lambda})]\theta_o ,$$

and that the pendulum period is modified to

$$P = 2\pi \left(\frac{\ell - \lambda}{g}\right)^{1/2} .$$

(iv) Finally show that the pendulum periods when swinging along $\mathbf{e}_x$ and $\mathbf{e}_y$ differ by

$$\frac{\delta P}{P} = \left(\frac{b-a}{\ell}\right)\left(\frac{1}{48\epsilon}\right)^{1/2} .$$

From this one can determine how accurately the two thicknesses a and b must be equal to achieve a desired degree of isotropy in the period. A similar analysis can be carried out for the more realistic case of a slightly elliptical wire.

****

10.7 Deformation of Plates — Keck Telescope Mirror

The world's largest optical telescopes, the two ten meter Keck telescopes, are located on Mauna Kea in Hawaii. It is very difficult to support traditional, monolithic mirrors so that they maintain their figure as the telescope slews because they are so heavy, and so a new method of fabrication was sought. The solution devised by Jerry Nelson and his colleagues was to construct the telescope out of 36 separate hexagons, each 0.9m on a side. However, this posed a second problem, grinding the reflecting surface of the mirror to the desired hyperboloidal shape. A novel technique called *stressed mirror polishing* was developed to accomplish this. This technique relies on the fact that it is relatively easy to grind a surface to a spherical shape, but technically highly challenging to create a non-axisymmetric shape. So, during the grinding, stresses are applied around the boundary of the mirror to deform it and a spherical surface is produced. The stresses are then removed and the mirror springs into the desired shape. Computing the necessary stresses is clearly a problem in classical elasticity theory and, in fact, is a good example of a large number of applications where the elastic body can be approximated as a thin plate.

Let us therefore modify our treatment of the bending of a narrow beam so that it is applicable to a thin elastic surface. In this example, the applied stress is so large that we can ignore gravitational forces (at least in our simplified treatment). We suppose that the mirror has a uniform thickness t and treat it as a circle of radius R. It is deformed as a result of a net vertical force per unit area F. This force is applied at the lower surface when positive and the upper surface when negative. In addition there are bending moments M applied around the rim of the mirror, just as happens at one end of the cantilever.

We follow a similar procedure and assume the existence of a neutral surface where the strain vanishes. We again assume the vertical displacement of the neutral surface, $\eta(x_i)$, where $x_i = \{x, y\}$ are orthogonal coordinates lying in the surface. The third coordinate, z, advances vertically upward from the neutral surface.) We relate the in-plane strain to the vertical displacement η as before,

$$\xi_{i,j} = -z\eta_{,ij} \tag{10.72}$$

[cf. Eq. (10.61)].

In order to compute the horizontal force density, we must relate the expansion θ to the horizontal strain. We do this by making a similar approximation to that made for the wire and the beam; we suppose that the vertical stress T_{zz} is small compared with the horizontal stress, T_{ij}. (We will verify our assumption below.) If we approximate it as zero, we obtain from Eq. (10.41)

$$T_{zz} = -K\theta - 2\mu\Sigma_{zz} = \frac{-E\theta}{3(1-2\nu)} + \frac{E}{(1+\nu)}(\xi_{i,i} - \frac{2}{3}\Theta) = 0\ . \tag{10.73}$$

where we have substituted Eq. (10.6), (10.45). (Remember the Einstein summation convention!) Solving for Θ,

$$\Theta = -\left(\frac{1-2\nu}{1-\nu}\right) z\nabla^2\eta\ , \tag{10.74}$$

where ∇^2 is the horizontal Laplacian, i.e. $\nabla^2\eta \equiv \eta_{,xx} + \eta_{,yy}$ Eq. (10.74) allows us to express the horizontal stress T_{ij} exclusively in terms of $\eta_{,ij}$ using Eq. (10.41).

$$T_{ij} = Ez\left[\frac{\nu}{(1-\nu^2)}\nabla^2\eta\ \delta_{ij} + \frac{\eta_{,ij}}{(1+\nu)}\right]\ . \tag{10.75}$$

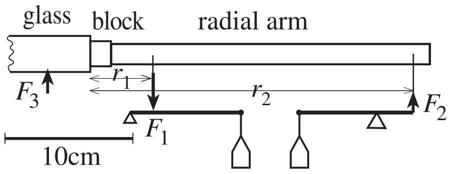

Fig. 10.9: Schematic showing mirror blank, radial arm and lever assembly used to apply shear forces and bending torques to the periphery of the mirror. F_1 need not equal F_2 as there is a pressure F_3 applied to the back surface of the mirror.

The analog of Eq. (10.63) for the horizontal force density is now

$$f_i = -T_{ij,j} - T_{iz,z} = -\frac{Ez}{1-\nu^2}\nabla^2\eta_{,i} - T_{iz,z} = 0\ . \tag{10.76}$$

Next we use the same trick we used for the cantilever, namely we multiply by z and integrate to obtain

$$\frac{Et^3}{12(1-\nu^2)}\nabla^2\eta_{,i} = \int_{-t/2}^{t/2} dz T_{iz}\ . \tag{10.77}$$

Now, instead of the total vertical shearing force, we use the vertical shear force density S_i acting vertically perpendicular to a line in the mirror, whose normal is in the direction i.

$$S_i \equiv \int dz T_{zi} = D\nabla^2\eta_{,i}\ , \tag{10.78}$$

where

$$D = \frac{Et^3}{12(1-\nu^2)} \tag{10.79}$$

is the flexural rigidity for a plate. (Analogous to Eq. (10.67) , we can define a bending torque density

$$M_{ij} \equiv \int dz z T_{ij} \tag{10.80}$$

substituting Eq. (10.75) .)

Finally, consider a small area of the mirror. The total vertical shearing force acting upon it is given by line integral of S_i around its boundary. Consequently, applying the divergence theorem, the vertical shear force per unit area is $S_{i,i}$ and this must be balanced by the net force density, F. The equation for elastostatic balance of a plate, the counterpart of Eq. (10.69) , is

$$\nabla^2(\nabla^2\eta) = F/D\ , \tag{10.81}$$

The static deformation of a thin plate must satisfy Eq. (10.81) subject to appropriate boundary conditions. We use it to justify our approximation that the vertical stress vanishes, for $T_{zz} \sim F = O(D\eta/R^4) = O(Et^3\eta/R^4) = O(t/R)^2 T_{ij}$.

The individual Keck mirror segments were constructed out of a ceramic material with Young's modulus $E = 89$GPa and Poisson's ratio $\nu = 0.24$ (cf. Table 2.1). A mechanical jig is constructed to apply shear forces and bending torques at 24 uniformly spaced points around the periphery of the mirror (Figure 10.9). The maximum stress is applied for the six outermost mirrors and is 2.4×10^6N m^{-2}, 12 per cent of the breaking tensile strength (2×10^7N m^{-2}).

****

EXERCISES

Exercise 10.11 *Practice: Keck Telescope*
Consider the lever assembly shown in Figure 10.9. Compute the applied shear forces and bending torques.

Exercise 10.12 *Example: Paraboloidal Mirror*
Show how to construct a paraboloidal mirror of radius R and focal length f by stressed polishing.

(i) By comparing the shape of a paraboloid to that of a sphere of similar curvature at the origin, show that required vertical displacement of the stressed mirror is

$$\eta(r) = \frac{r^4}{64 f^3} ,$$

where r is the radial coordinate and we only retain terms of leading order.

(ii) Hence use Eq. (10.81) to show that a uniform force per unit area

$$F = \frac{D}{f^3} ,$$

where D is the Flexural Rigidity, must be applied to the bottom of the mirror. (Ignore the weight of the mirror.)

(iii) Hence show that if there are N equally-spaced levers attached at the rim, the vertical force applied at each of them is

$$S_{zr} = \frac{\pi D R^2}{N f^3}$$

and the associated bending torque is

$$M = \frac{\pi D R^3}{2 N f^3} .$$

(iv) Show that the radial displacement is

$$\xi_r = -\frac{r^3 z}{16 f^3} ,$$

where z is the vertical distance from the neutral surface, halfway through the mirror.

(v) Hence evaluate the expansion Θ and the components of the strain tensor $\mathbf{\Sigma}$ and show that the maximum stress in the mirror is

$$T_{\rm max} = \frac{(3-2\nu)R^2hE}{32(1-2\nu)(1+\nu)f^3} ,$$

where h is the mirror thickness. Comment upon the limitations of this technique for making a thick, "fast" (i.e. $2R/f$ large) mirror.

Exercise 10.13 *Practice: Biharmonic Equation*
A uniform, isotropic, elastic solid is in equilibrium under gravity and surface stress. Use Eq. (10.35) to show that the displacement $\boldsymbol{\xi}(\mathbf{x})$ is biharmonic, i.e. it satisfies the differential equation

$$\nabla^2\nabla^2\boldsymbol{\xi} = 0 .$$

Show also that the expansion Θ satisfies

$$\nabla^2\Theta = 0 .$$

****

10.8 Bifurcation - Mountain Folding

So far, we have considered stable elastostatic equilibria, and have implicitly assumed that the only reason for failure of a material is exceeding the elastic limit. However, anyone who has built a card house knows that mechanical equilibria can be unstable and that this can have unfortunate consequences. One large scale example is furnished by the formation of mountains. The surface of the earth is covered by several interlocking "plates" that move over the earth's surface and are driven into each other by slow, convective motions in the underlying mantle. As we have already mentioned in this section, it takes roughly a hundred million years for this to happen. When plates are pushed together, mountains may be formed. Two ways in which this can occur are by *folding* (e.g. the Jura Mountains of France) which sometimes happens when a portion of crust is compressed in one direction and by forming *domes* (e.g. the Black Hills of Dakota) which arise when there is simultaneous compression along two directions.

To make a simple model of folding, take a new playing card and squeeze it between your finger and thumb (Figure 10.10). When you squeeze gently, the card remains flat, but as the force applied to the ends of the card is increased, the card suddenly "buckles" and adopts a curved shape, the curvature increasing rapidly with the applied force. If a larger force is applied, then it is possible to find equilibrium states of "higher quantum number", i.e. with one or more nodes in the transverse displacement of the card.

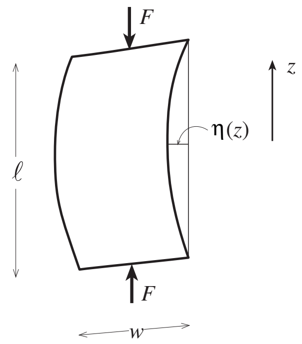

Fig. 10.10: A playing card of length l, width w and thickness t is subjected to a compressive force F, applied at both ends. The ends of the card are fixed but are free to pivot.

Let us first describe the physics of the playing card. We designate the transverse displacement of the card η as a function of distance z from the mid-point. We suppose that the ends of the card are free to pivot but not move, so

$$\eta(\pm\ell/2) = 0\ . \tag{10.82}$$

For small displacements, the bending torque is

$$M(x) = D\frac{d^2\eta}{dz^2}\ , \tag{10.83}$$

where $D = wt^3E/12$ is the flexural rigidity (cf. Eq. (10.66)). As the card is very light, the total torque acting on a section of the card from z to one end is the bending torque applied at z plus the torque associated with the applied force $F\eta$ and this must vanish. Therefore

$$D\frac{d^2\eta}{dz^2} + F\eta = 0\ . \tag{10.84}$$

The eigenfunction solutions of Eq. (10.69) satisfying boundary conditions (10.82) are

$$\eta = \eta_0 \cos kz\ , \tag{10.85}$$

where

$$k = \left(\frac{F}{D}\right)^{1/2} = \frac{n\pi}{\ell} \tag{10.86}$$

So, there is a critical force given by

$$F_{crit} = \frac{\pi^2 wt^3 E}{12\ell^2}\ , \tag{10.87}$$

below which there is no solution except $\eta = 0$. By contrast, when the applied force is equal to F_{crit} the solution (10.85) is indeterminate; in the linear approximation, all values of ξ_0 are equally good. This is the sign of a bifurcation. A full discussion requires elastodynamics,

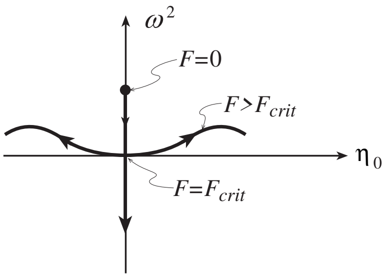

Fig. 10.11: Schematic illustration of the behavior of the frequency of small oscillations about equilibrium and the displacement of the center of the card, η_0. Equilibria with $\omega^2 > 0$ are stable; those with $\omega^2 < 0$ are unstable. The applied force F increases in the direction of the arrows.

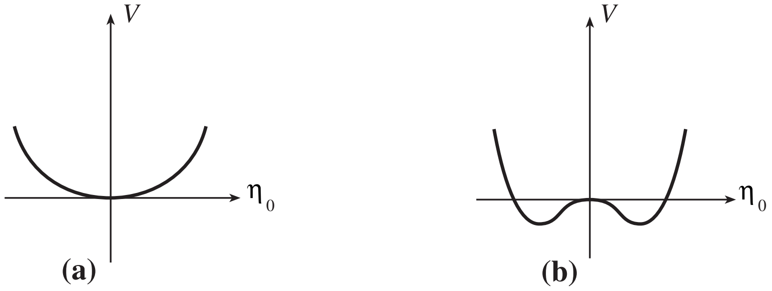

Fig. 10.12: Representation of bifurcation by a potential energy function $V(\xi_0)$. a) When the applied force is small, there is only one stable equilibrium. b) As the applied force F is increased, the bottom of the potential well flattens and eventually the number of equilibria increases from one to three, of which only two are stable.

but basically what happens is that if we consider the behavior of small perturbations about equilibrium, then for forces $F < F_{crit}$, the perturbations decay exponentially. When $F = F_{crit}$, the card is neutrally stable. However, when $F > F_{crit}$, straight cards constitute unstable equilibria. There is a however a unique stable equilibrium with a central displacement η_0 that increases rapidly with increasing F. However, to find it requires including non-linear terms in the equation of elastostatic equilibrium.

There is another way of looking at bifurcations. Let us consider possible states labeled by the displacement of the midpoint, η_0. For each value of η_0, we choose the solution that satisfies elastostatic equilibrium $\eta > 0$ and $\eta < 0$. We can then define a general potential energy $V(\eta_0)$ for the system and associate the equilibria with its stationary points. (Figure 10.12.) At small values of the force, the potential energy has a only one minimum corresponding to a single stable equilibrium. However, as the force is increased, the potential minimum flattens out until an additional maximum and minimum are created. We can regard this as adding a quartic term of increasing strength to the normal simple harmonic potential. In this case, the maximum is the unstable, zero displacement equilibrium and the two minima are the two stable finite amplitude equilibria. This procedure of representing a continuous system with an infinite number of degrees of freedom by a few coordinates and finding the equilibrium by minimising a potential is quite common. Coordinates like η_0 are sometimes called *state variables*, and physical parameters like the force F are then called *control variables*. The bifurcation is an example of a *cusp catastrophe*; it is an analog of the catastrophes we met in geometrical optics.

Other examples of bifurcations include the failure of struts under excessive compressive loads, the instability (or *whirling*) of a drive shaft when it rotates too rapidly, and the development of triaxiality in self-gravitating fluid masses (i.e. stars) when their rotational kinetic energy becomes comparable with their gravitational energy.

Let us now return to the problem of folding mountains with which we began this section. Our physical model is clearly inadequate to describe the full phenomenon as we have omitted gravitational forces and the restoring force associated with the underlying *mantle*. The former causes no difficulties of principle as it just changes the equilibrium state. The latter can be modeled by treating the Earth's mantle as a viscoelastic medium. When it departs from equilibrium it changes not on a dynamical time, the time for a seismic wave to cross it, of order minutes, but instead the time for the underlying rocks to flow, typically millions of years. Despite these limitations it is possible to understand semi-quantitatively why plates of rock ($E \sim 100$GPa, $\nu \sim 0.25$), buckle when subject to large horizontal compressive forces.

****

EXERCISES

Exercise 10.14 *Practice: The Height of Mountains*
Estimate the maximum size of a mountain by requiring that the shear stress in the underlying rocks not exceed the elastic limit. Compare your answer with the height of the tallest mountains on Earth.

Exercise 10.15 *Example: Neutron Star Crusts*
The crust of a neutron star is made of iron ($A = 56, Z = 26$) at density ρ. It is supported against the pull of gravity by the pressure of a relativistic, degenerate, electron gas.

(i) Show that the electron Fermi energy is given by

$$E_F = (3\pi^2 n_e)^{1/3}\hbar c \ ,$$

where $n_e = Z\rho/Am_P$ is the free electron density. Hence show the Fermi pressure is given by

$$p_F = \frac{1}{4} n_e E_F \ .$$

(ii) Use the definition of Bulk Modulus preceding Eq. (10.34) to express it in the form

$$K = \frac{1}{3} n_e E_F$$

(iii) The iron ions are arranged in a *body centered cubic* lattice so that they have a shear modulus. Show that

$$\mu = C \left(\frac{n_e}{Z}\right)^{4/3} Z^2 e^2 \ ,$$

where C is a numerical constant of order unity. Hence show that the ratio of the shear modulus to the bulk modulus is

$$\frac{\mu}{K} = \left(\frac{3}{\pi}\right)^{2/3} C Z^{2/3} \left(\frac{e^2}{\hbar c}\right) .$$

Do you expect there to be large mountains on the surfaces of neutron stars?

****

Bibliography

Braginsky, V. B., Gorodetsky, M. L., and Vyatchanin, S. P. 1999. "Thermodynamical fluctuations and photo-thermal shot noise in gravitational wave antennae" *Physics Letters A*, **264**,1.

Braginsky, V., Mitrofanov, M. and Panov, V. 1984. *Systems with Small Dissipation*, Chicago: University of Chicago Press.

Chandrasekhar, S. 1962. *Ellipsoidal Figures of Equilibrium*, New Haven: Yale University Press.

Jackson, J. D. 1999. *Classical Electrodynamics*, New York: Wiley.

Landau, L. D., and Lifshitz, E. M. 1970. *Elasticity*, Oxford: Pergamon.

Levin, Yu. 1998. "Internal thermal noise in the LIGO test masses: a direct approach" *Physical Review D*, **57**,659–663.

Liu, Y. T., and Thorne, K. S. 2000. "Thermoelastic noise and thermal noise in finite-sized gravitational-wave test masses" *Physical Review D*, in preparation.

Mathews, J. and Walkder, R. L. 1965. *Mathematical Methods of Physics*, New York: Benjamin.

Messiah, A. 1962. *Quantum Mechanics, Vol. II*, North-Holland, Amsterdam.

Southwell, R. 1963. *Elasticity.*

Thorne, K.S. 1980. "Multipole Moments in General Relativity" *Rev. Mod. Phys.*, **52**, 299.

Turcotte, D. L. and Schubert, G. 1982. *Geodynamics*, New York: Wiley.

Timoshenko, S. and Goodier, J. N. 1970. *Theory of Elasticity*, New York: McGraw-Hill.

Yeganeh-Haeri, A., Weidner, D. J. & Parise, J. B. 1992. *Science*, **257**, 650.